RSRE
MEMORANDUM No. 4564

ROYAL SIGNALS & RADAR ESTABLISHMENT

LASER DIODE END-PUMPED Nd:YAG LASER

Author: I F Elder

PROCUREMENT EXECUTIVE,
MINISTRY OF DEFENCE,
RSRE MALVERN,
WORCS.

CONDITIONS OF RELEASE

0121005 309213

.....

DRIC U

.....

DRIC Y

Reports quoted are not necessarily available to members of the public or to commercial organisations.

DISCLAIMER NOTICE

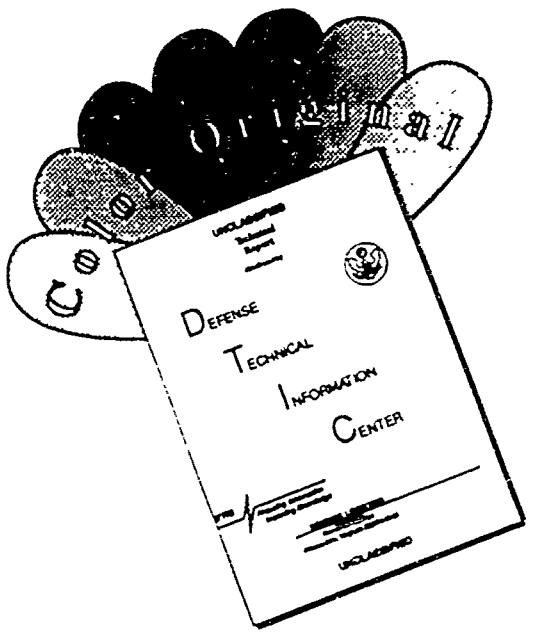

THIS DOCUMENT IS BEST QUALITY AVAILABLE. THE COPY FURNISHED TO DTIC CONTAINED A SIGNIFICANT NUMBER OF COLOR PAGES WHICH DO NOT REPRODUCE LEGIBLY ON BLACK AND WHITE MICROFICHE.

DEFENCE RESEARCH AGENCY

RSRE Memorandum No 4564

Title: **LASER DIODE END-PUMPED Nd:YAG LASER**

Author: **Ian F Elder**

Date: **January 1992**

ABSTRACT

100 Hz operation of a Nd:YAG laser longitudinally pumped by a 1 W peak power quasi-cw laser diode was investigated theoretically and experimentally. An optical-to-optical slope efficiency of 33%, indicating a wall-plug efficiency of 7%, was exhibited, but the threshold optical power of 330 mW was high due to poor antireflection coatings on the laser rod giving a round-trip intracavity loss of 3.1%. The 1.064 μm output was observed to be diffraction-limited. The theoretical modelling of the laser's input/output characteristics agreed well with the experimentally obtained results.

CONTENTS

§1: INTRODUCTION

1.1: A Brief History of Diode-Pumping

The first use of semiconductor sources to pump a solid-state laser was in 1963, when Newman used 880nm light from incoherent GaAs LEDs to excite Nd:$CaWO_4$ [1]. Laser action was observed in a gallium arsenide diode by Hall et al. in 1962 [2].

Early progress in diode laser-pumped solid-state lasers was limited by the need for cryogenic cooling, and by the low powers of the diode lasers. The first pumping of a solid-state laser using laser diodes, reported in 1964 by Keyes and Quist [3], involved transversely pulse-pumping a U^{3+}:CaF_2 crystal rod, with the entire laser enclosed within a liquid helium-filled dewar. Longitudinal pumping was demonstrated in 1973 by Chester and Draegert [4] using a GaAsP LED to pump a Nd:YAG rod.

The early work in the 1960s on diode-pumped solid-state lasers (DPSSLs) soon concentrated on neodymium-doped crystals, one of the principal reasons being that this trivalent rare earth ion possesses strong absorption in the emission bands of GaAs, AlGaAs and GaAsP LEDs and diode lasers [5]. Ross [6] demonstrated the first diode-laser pumped Nd:YAG laser in 1968, using a single GaAs diode in a transverse geometry. Conant and Reno [7] recognised that the higher brightness of diode lasers over LEDs would mean that the pump radiation could be absorbed in a smaller volume, leading to higher gain and lower threshold. This early work on diode-pumping was restricted to pulsed operation due to the limitations of the diodes themselves. It was not until 1972, nearly a decade after the pioneering experiments, that Danielmeyer and Ostermeyer [8] demonstrated room temperature diode laser-pumping of Nd:YAG. Room temperature cw operation was first demonstrated in 1976 [9].

The upsurge of interest in DPSSLs in the 1980s came about due to the development of high power laser diode-arrays by Scifres et al. in 1982 [10], leading to higher brightness and greater intensity sources. Solid-state laser development has been paced by the improvement and discovery of pump sources, right from the early days of using helical flashlamps with ruby, onto the linear flashlamp and arclamp almost universally in use today, and onto the new semiconductor-based pump sources. Progress in diode laser array technology has been rapid. The ability to grow thin layers of material accurately has led to the construction of quantum well devices, with low thresholds and much improved thermal performance. Arrays consisting of centimetre bars of emitters are now available commercially, capable of producing up to 60W peak power in 200μs pulses, or 20W cw[11] . These bars can then be packaged in "rack-and-stack" fashion to produce 2D arrays of emitters. The removal of waste heat from the light emitting regions (thermal management) is one of the major design problems to be tackled. There has been much emphasis on lasers based on neodymium-doped crystals and glasses, taking full advantage of the capabilities offered by laser diode pump sources. In addition improved diode technology has initiated work on lasers using other rare earths as the active ion, principally erbium, thulium and holmium.

A thorough review of the diode-pumping issue is the subject of several excellent articles [5,12,13].

1.2: Advantages Offered by Diode-Pumping

It is instructive to make a comparison of flashlamps and laser diodes/laser-diode arrays as actual pump sources for solid-state lasers. The diode laser efficiently emits optical radiation into a narrow spectral band. When this emission wavelength lies within the absorption band of the active ion of the solid-state laser medium, diode laser optical pumping can be very efficient with little excess heat generation. Flashlamps, although they convert electrical energy to optical energy more efficiently (80% rather than 30-50% [13]), they do so over a wide spectral band, and so the absorption efficiency is very much lower. The substantial UV content of flashlamp light can lead to degradation of the pump cavity and coolant, and solarisation of the laser rod, problems which are eliminated with laser diode pump sources. A good spectral match between pump wavelength and laser medium absorption band(s) also significantly reduces the amount of waste heat generated in the laser medium e.g. with diode-pumped Nd:YAG, lattice heating is reduced by a factor of three compared with a flashlamp-pumped system [14] .

A significant advantage of laser diode pumping compared with flashlamp-pumping is system lifetime and reliability. Laser diode arrays have exhibited lifetimes of the order of 20,000hrs in cw and 10^9 shots in the pulsed mode; flashlamp life is of the order of 200hrs cw and 10^7 shots in pulsed operation [15]. The laser diode is a much stabler source than the flashlamp, hence DPSSLs show increased frequency stability and decreased linewidth than their flashlamp-pumped equivalents c.f. a lamp-pumped system linewidth of 120kHz [16] , and a DPSSL frequency stability of <1kHz in 1ms [17]. Flashlamps require large (high voltage) power supplies, storage capacitors and trigger circuits, and so are bulky and inherently more dangerous than the relatively compact low voltage supplies used to power laser-diode arrays.

Higher average powers can presently be obtained from lamp-pumped systems. However scaling to higher average powers for diode-pumped systems is on the increase, with improvements in diode fabrication and thermal management technology. Another hindrance is cost, with diode laser arrays being much more expensive than flashlamps, but prices are on a downward trend as sales volumes increase.

Another question often asked is "Why use the laser diode to pump another solid-state laser instead of using the diode directly ?" The diode laser is essentially a cw device with low energy storage capability due to a short upper state lifetime, whereas the solid-state laser can store energy in the long-lived metastable ion levels, leading to enhanced peak powers through Q-switching. The geometry of the edge-emitting diode laser, where the radiation originates from a very small facet area, leads to a low brightness beam of high divergence. The emitting aperture is typically rectangular, leading to differing divergences in the two orthogonal directions. If focussed into a

solid-state laser medium, a diffraction-limited high brightness beam can be generated. Because of their short cavity length (typically less than 1mm) diode lasers have much larger linewidths than diode-pumped lasers. In order to reduce linewidth, the laser diode has to be placed in an external cavity, leading to added complexity. Finally, diode-pumped solid-state lasers offer the possibility of operation in wavelength regions where laser diodes either perform poorly or are not available.

§2: SPECTROSCOPY OF Nd:YAG

The active ion in Nd:YAG is the trivalent rare earth ion neodymium. The neodymium atom has an outer electron configuration $5s^25p^64f^35d^16s^2$, with the trivalent ion giving the $5d^16s^2$ electrons to make ionic bonds. The energy levels of the incompletely filled 4f shell spread over approximately 40,000cm^{-1}, with many energy levels separated by 10-20,000cm^{-1}, giving rise to optical photons from the near infrared to the blue [18].

These 4f electrons are shielded by the outer 5s,5p electrons from the ionic lattice, and so are weakly affected by vibrations. Hence neodymium (and other rare earth) spectra are characterised by sharp lines, resembling those of the free ion. The crystal field removes the orbital degeneracy of the levels, since the ion is no longer in a spherically symmetric potential, and so the levels are split. However, due to the weak electron-phonon coupling, this splitting is small compared with the energy level separations of the free ion. These sharp spectral features are thermally broadened at room temperature.

Neodymium-doped YAG (yttrium aluminium garnet) possesses a number of properties favourable for laser operation, and is by far the most widely-used solid-state laser material. Pure YAG ($Y_3Al_5O_{12}$) is a colourless, optically isotropic crystal, possessing a cubic structure typical of garnets [19] . In YAG the Nd^{3+} ion substitutes for the Y^{3+} ion - both are trivalent, so charge compensation is not required. The radii of the two rare earths differ by about 3%. This limits the neodymium concentration to 1.5% of the yttrium, above which crystal strain occurs. The YAG host is hard, of good optical quality and has a high thermal conductivity, all advantageous characteristics for a solid-state laser medium.

The energy level diagram for Nd:YAG is shown in figure 1. The neodymium ions exhibit fluorescence of narrow spectral linewidth, such that the corresponding laser transitions can benefit from a high stimulated emission cross-section, hence low pump thresholds, suggesting the use of laser diodes. Pumping with laser diodes emitting near 809nm excites Nd^{3+} from the $^4I_{9/2}$ ground state manifold to the pump bands of the $^4F_{5/2}$ and $^2H_{9/2}$ manifolds. The absorption spectrum of Nd:YAG around 809nm is shown in figure 2.

The excited ions then emit nonradiatively, decaying rapidly to the metastable $^4F_{3/2}$ level, which has a fluorescence lifetime of 230μs at room temperature, for a 1% doped sample. This itself consists of two levels, labelled R_1 and R_2, separated by approximately 80cm^{-1}. These two levels are in thermal equilibrium, with rapid replenishment between them maintaining a Boltzmann distribution. At room temperature, the excited state population is distributed such that 60% is in R_1, 40% in R_2.

The laser wavelength with the highest transition probability is the 1.064μm line, from the R_2 level to the third level of the $^4I_{11/2}$ manifold, 2111cm^{-1} above the ground state. Hence at room temperature the terminal laser level has a negligible population, approximately exp(-10) of the

ground state. With a rapid nonradiative decay (lifetime 30ns) from the terminal laser level, Nd:YAG can be regarded as a four-level laser. Koechner [19] quotes a value of 6.5×10^{-19} cm^2 for the stimulated emission cross section of 1% doped Nd:YAG at 1.064μm, and a laser linewidth of 0.45nm.

§3: SEMICONDUCTOR LASERS

3.1: Introduction

In a laser diode, the p-n junction provides the active medium. To meet the requirements for laser action, a population inversion and optical feedback must be present [20]. Light emission occurs by recombination of electron-hole pairs in the p-n junction region. By heavily doping the p- and n-type regions, and applying a forward bias voltage greater than the bandgap across the junction, sufficient population builds up to generate an inversion, leading to gain proportional to the number density of the electron-hole pairs. With resonant optical feedback provided by the cleaved facets of the crystal, laser emission will occur when the available gain exceeds the loss.

The diode in which laser action was first demonstrated was a homojunction diode of gallium arsenide (GaAs) in which the active layer was formed at the junction between n-type and p-type layers of the same semiconductor [19]. Improved laser performance was subsequently exhibited by the double heterostructure laser diode, in which the active layer was sandwiched between layers of greater bandgap energy. These outer layers of gallium aluminium arsenide (GaAlAs) improved the confinement of both the optical field and the charge carriers in the plane parallel to the p-n junction. The introduction of a particular fraction of aluminium into the GaAs active layer allows the bandgap of the lasing transition to be specified. Fine control of the bandgap energy and hence the lasing wavelength can be achieved by controlling the operating temperature of the laser diode. This temperature dependence leads to chirping of the output wavelength when operated in pulsed mode.

The next step in development concerned charge and flux confinement in the plane perpendicular to the p-n junction. The lateral extent of laser action in this plane may be controlled by gain guiding, where a metallic contact stripe on the upper layer of the device defines the width of carrier diffusion and hence the gain width. A further breakthrough towards high power laser diodes suitable as pump sources for DPSSLs was the development of quantum-well structures. Here the active layer thickness is typically less than 30nm, the de Broglie wavelength of an electron. Quantisation of the allowed energy states in the conduction and valence bands occurs, determined by the layer thickness. This provides another route to controlling the bandgap energy, in addition to adding different dopants to the active layer semiconductor. The resultant quantisation of energy levels enhances carrier recombination, with the consequence that threshold currents of quantum-well lasers are substantially lower than for conventional "bulk" semiconductor lasers. This reduces the heating of the device, so that higher output powers can be achieved without sacrificing diode lifetime.

Using a stripe geometry, laser-diode arrays consisting of several emitters can be fabricated. If the stripe-to-stripe spacing is sufficiently small the individual emitters become phase-locked, resulting in a good quality output beam. For diode-pumping, where the principal concern is maximum light output possible, such phase-locking is unnecessary, and incoherent arrays suffice. These have an optically insulating layer between the active stripes. Therefore each stripe represents an

independent layer, and so many stripes can be placed on the same substrate, whereas with phase-locked coherent arrays, the total width cannot exceed a certain limit otherwise lateral lasing will occur.

A series of arrays can be fabricated on a wafer of substrate to produce laser diode-bars. Usually these bars have a packing density or "fill factor" of up to 30% to allow effective thermal control of the emitters. Such devices, in the form of centimetre bars, are available commercially from several sources.

3.2: Characterisation of Laser Diodes

The series of experiments performed in this report were carried out using laser diodes supplied by Northern Telecom Europe (formerly STC).

These devices were 1W peak power diodes, operated with 200μs current pulses at 100Hz, a 2% duty cycle. For pulses longer than a few microseconds, a state of thermal equilibrium is approached, and so this long-pulse pumping regime is referred to as "quasi-cw".

The laser diode was a GaAs/AlGaAs structure and had an active region consisting of two quantum wells, each of thickness 10nm, with a cavity length of 500μm. This was a multielement (array) stripe geometry device, with a dozen 5μm emitters on an 8μm pitch making up the 100μm wide output facet. The diode was bonded p-side down (for improved heatsinking) on a TO-18 style package, with the facet open to the atmosphere. This package was then mounted on a copper heatsink, and the diode connected to its power supply. Using a Gentec ED200 pyroelectric joulemeter with an EDX-1 amplifier, the light output of the diodes was tested against the drive current (the L/I characteristic). The result is shown in figure 3, which indicates a threshold current of 0.3A and a slope of 0.83W/A, implying an external quantum efficiency (number of output photons to number of electrons supplied) of 55%, in agreement with the data supplied with the diodes. Figure 4 shows the voltage/current characteristic, indicating a breakover voltage of 1.5V corresponding to the semiconductor bandgap, and a total device resistance of 0.4Ω. Knowing the voltage and current supplied to the diode, the electrical-optical conversion efficiency can be derived. Figure 5 shows the optical power versus electrical power curve, which has a differential slope of 35%. Calculating the efficiency of conversion for a series of drive currents results in figure 6. A maximum efficiency of 31% is reached for currents above 1A , corresponding to at least 600mW of pulsed light. Above 1.5A (1W), the light output efficiency of the laser diode starts to fall away as the diode is driven too hard.

Unfortunately the wavelength and spectral width of these pumping diodes could not be measured, as a monochromator was not available. The data supplied indicated that the devices emitted 807nm

light at room temperature with a spectral width of 1nm. The optical chirp through the 200μs current pulse was stated as being 2nm. This chirping is due to the thermally induced change in the bandgap of the GaAs wells as the current pulse is applied. The active region heats up, reducing the bandgap and so shifting the output to longer wavelengths. A smaller effect on the spectral output is due to the fact that as large numbers of charge carriers are injected into the active region. the refractive index, hence the cavity length, undergo change, in turn modifying the longitudinal mode structure.

The laser diodes produced a dual-lobed far-field intensity distribution, with full width at half maximum (FWHM) divergence of 10° by 30°, the higher divergence being in the plane perpendicular to the active region layer. being the smaller dimension of the output facet. The laser diode light was plane polarised in the horizontal direction i.e. in the plane of the active region layer.

§4: THEORY OF PULSED LASER OPERATION

The fact that the Nd:YAG laser medium is being pumped by a pulsed light source with a pulse duration less than the fluorescence lifetime of the upper laser level means that the temporal behaviour of the solid-state laser output will depend very much on the pump power, especially close to threshold. Modelling of this dependence is necessary in order to check the validity of the experimental results.

The laser diode used in the experiments was injected with a rectangular current pulse, and gave an optical output of similar waveform. At drive currents above 1A, the light output waveform started to droop towards the end of the current pulse. This was attributed to the additional heating of the laser diode at these larger current densities. In order to model this system, it is assumed that the pump light has a rectangular waveform, and that there is no saturation of the gain medium.
Consider a rectangular pulse of duration T_p and energy E_p.

$$\therefore \text{ Pump power } P_p = E_p/T_p$$

For a pulse of duration t, the stored energy E_{st} in the laser medium (below threshold) is given by an expression of the form

$$E_{st} = \int P_p \exp(-t'/\tau)dt' \qquad \{0,t\}$$

where τ is the spontaneous lifetime of the upper laser level.

$$E_{st} = P_p \tau (1- \exp(-t/\tau))$$
$$t = -\tau\ln(1- E_{st}/P_p.\tau)$$

At threshold the pump energy creates sufficient excitation to allow lasing at the very end of the pump pulse. In this case

$$T_p = -\tau\ln(1- E_{th}/P_{p,th}.\tau)$$
$$= -\tau\ln(1- E_{th}.T_p/E_{p,th}.\tau)$$

Threshold excitation E_{th} is that which generates an inversion threshold, and also overcomes cavity losses, such that the round-trip gain in the laser cavity is unity. When the pump energy is increased above the threshold value, threshold excitation is reached at a time T_1 which is less than T_p and excitation is instantaneously available for lasing, until the end of the pump pulse at time T_p. Assuming that the energy extraction by lasing takes place very quickly, the intracavity laser energy E_l (and hence the laser output energy) is given by an expression of the form

$$E_l = \int (P_p - P_{p,th})dt' \qquad \{T_1,T_p\}$$
$$= (1/T_p)(E_p - E_{p,th})(T_p - T_1)$$
$$= (1/T_p)(E_p - E_{p,th})[T_p + \tau\ln(1- E_{th}.T_p/E_{p,th}.\tau)]$$

Eliminating the unknown quantity E_{th} yields the following expression

$$E_l = (E_p - E_{p,th})[1 + (\tau/T_p)\ln(1 - (E_{p,th}/E_p)(1 - \exp(-T_p/\tau))]$$

Normalising to the pump threshold energy implies

$$E_l/E_{p,th} = [(E_p/E_{p,th}) - 1]\,[1 + (\tau/T_p)\ln(1 - (E_{p,th}/E_p)(1 - \exp(-T_p/\tau))]$$

For the case of diode-pumped 1% doped Nd:YAG

$T_p = 200\mu s$

$\tau = 230\mu s$ (at room temperature)

The graph of normalised laser output energy versus normalised pump energy is shown in figure 7. It shows that close to threshold there is marked curvature in the output energy behaviour before it tends to a straight line. This phenomenon can be explained by looking at the variation of the Nd:YAG laser pulse as a function of pump energy. The theory gives an expression for the time T_1 at which lasing threshold is reached. Hence the laser pulse duration T_{las}, for a rectangular pump pulse, is

$$T_{las} = T_p - T_1$$
$$= (200 - T_1)\mu s$$

This is graphed in figure 8. The pulse length increases very rapidly until twice the threshold pump energy is attained, and then the rate of increase starts to level off. Therefore close to threshold the energy extracted by lasing is reduced by the short laser pulse lengths involved.

It is instructive to calculate the normalised laser output power using the energy and pulse length data tabulated in the appendix, then to plot this against the normalised pump power, as in figure 9. This clearly shows a linear dependence at all values of the pump power above threshold. With a rectangular pump pulse, pump power is supplied linearly to the laser medium. The laser output follows this behaviour, since excitation is continually replenished linearly above threshold. This result also confirms that the transfer of pump energy to laser output occurs rapidly relative to the fluorescence lifetime of the upper laser level. Hence this laser power output analysis can be equated with cw pumping of the laser medium, where threshold effects are not present.

The energy and power graphs derived here indicate that far above threshold the output power/energy tend to the corresponding pump values. This is an unphysical result, and in order to compare the theoretical data with experimental values, the following scaling factors need to be included when calculating the laser output power/energy:-

(1) The quantum defect between the pump (809nm) and lasing (1064nm) wavelengths. (This was ignored in the preceding analysis simply to ease the algebra)

(2) The efficiency with which excited ions reach the upper laser level and then contribute to lasing. Kaminskii [21] gives a value for this fluorescence efficiency of 0.995.

(3) The transmission of the optics between the laser diode and the laser medium.

(4) The efficiency of absorption of the pump radiation in the laser medium.

(5) The useful output coupling, which depends on the value of the output coupling and the intracavity loss.

§5: EXPERIMENTAL ARRANGEMENT

The basic layout of the diode-pumped Nd:YAG laser used in these experiments is shown in ıre 10. Longitudinal, or end-pumping, was employed as this offers the possibility of good spatial overlap between the pump beam and the laser mode of the Nd:YAG resonator, leading to a high efficiency system.

The diode power supply consisted of a twin +5,+20V unit powering a box containing the TTL logic controlling the current pulse width and frequency, and also the components delivering the current to the diode. A 0.1Ω monitor resistor allowed the drive current to be viewed on an oscilloscope. The laser diode package was mounted on a water-cooled copper heatsink. The water temperature could be set between 5 and 40°C, with an accuracy of ±0.1°C, using a Conair Churchill circulator unit.

In order to get good overlap between the pump beam and the resonator mode, the principal obstacle to overcome is to somehow collect and couple the highly divergent and elliptical output of the laser diode into the laser medium. There are several established techniques for achieving this; the one used here involved an anamorphic prism pair. The diode output was collimated with a 6.5mm focal length lens, before entering a holder containing the anamorphic prism pair. The input face of the first prism was set at Brewster's angle, so that there was zero insertion loss for the plane polarised diode radiation. The prisms are mounted such that the angle between their input faces effectively expands the pump beam in the horizontal (low divergence) direction with no effect on the vertical dimension. The light is then focussed into the Nd:YAG sample with a 25.6mm focal length lens. The ratio of collimating lens focal length to focussing lens focal length is nearly 1:4, so without the anamorphic prism pair present, there would be a magnification factor of four of the diode output facet by this lens system. The prisms are set to produce a fourfold expansion in the horizontal plane, and therefore the overall effect of the collecting optics used is to nullify the effect of the lenses in the horizontal plane. This helps to "circularise" the focussed pump spot to give better mode-matching with the circular TEM_{00} fundamental transverse mode of the Nd:YAG resonator.

The basic resonator consisted of three elements, two mirrors and a gain medium. The input dichroic mirror was 95% transmitting around 809nm, and 100% reflecting at 1064nm. This mirror had a 50cm radius of curvature. The laser medium used was an antireflection coated (nominally at both pump and laser wavelengths) 5mm long 1% doped Nd:YAG sample. Three different output couplers were used. All were plane mirrors, with transmissions 0.05%, 0.7% and 4.1% as measured on a Perkin-Elmer 39 spectrophotometer. A narrow-band 1064nm filter, with maximum transmission 25%, was placed in front of the output coupler to block out any unabsorbed pump light.

In this experimental set-up, the collecting optics, the input mirror and laser rod, and the output coupler were all mounted on separate translation stages, in order to provide several degrees of freedom when aligning the laser. A HeNe laser was set up at the opposite end of the optical table to provide initial alignment of the resonator. In order to fine tune the set-up to produce maximum output power in the TEM_{00} mode, the following procedure was adopted. After aligning the mirrors and rod with the HeNe, the laser diode current was set to produce at least 500mW of light. From the literature this was known to be far greater than the threshold power needed for end-pumped Nd:YAG. Laser output, if any, was observed using Cohu silicon CCD TV camera, connected via a frame-grabber to a PC running BigSky laser diagnostic software. This allowed the the spatial profile of the Nd:YAG output to be observed in real time, and as such was an invaluable tool in setting up the diode-pumped laser. Figure 11 shows how the beam profile altered as the resonator mirrors were finely adjusted, from the initial high threshold multimode operation of the misaligned cavity to the fundamental transverse mode. Once TEM_{00} mode operation was established, the pulse energy was then observed using an energy meter. Optimisation of the output energy could be achieved by several nonindependent methods:-

(a) Vertical and horizontal adjustment of the collecting optics (as a unit)

(b) Vertical and horizontal adjustment of the mirrors and the laser rod

(c) Tilt adjustments of mirrors and laser rod

(d) Translation of rod along resonator axis

(e) Temperature tuning of laser diode

As one is concerned here with the spatial overlap of a pump spot and resonator mode size both of submillimetre dimensions, the output energy was extremely sensitive to adjustments of the mirrors, and even more so to movement of the coupling optics. Temperature tuning of the diode, and adjustment of the laser rod position, allowed optimisation of the pump absorption, and thus provided an additional method of increasing the laser output. With the components used, the shortest resonator length possible was 8cm. The output coupler was also moved, opening up the resonator to a maximum length of 24cm, approaching a semiconfocal configuration (since the curved mirror had a 50cm radius of curvature).

§6: EXPERIMENTAL RESULTS

6.1: Focussing of Pump Light

Using the Cohu camera, the focussed light from the collecting optics was observed. The highly divergent dual-lobed diode radiation focussed to a spot 500µm by 200µm in diameter, approximately 20mm distance from the final surface of the focussing lens, in agreement with the manufacturer's data. However, the focus was astigmatic, with the horizontal 500µm focus occurring approximately a millimetre before the vertical 200µm focus. This effect could be due to a slight misalignment in the optics, or due to astigmatism in the diode output itself. Beyond the focal region, the p p light was once again highly divergent, around 12° by 15° FWHM.

In order to model the effect of the input mirror, and the laser rod itself, on the focussed pump beam, BEAM4 ray-tracing sortware was employed. This provided a geometrical analysis, and so there was no information on the size of the focussed spot. There was also no way in which to model the astigmatism. The particular experimental set-up used meant that the dichroic mirror and the laser rod were fixed at 5mm apart, but both could be moved as a unit relative to the focussing lens.

Figures 12 to 15 show the effect of moving the mirror/rod combination. At 85mm separation, the focus is right at the facet of the Nd:YAG sample. For end-pumping, it is required to couple the pump light efficiently into the TEM_{00} mode volume. Since the pump light is highly divergent, and the absorption length in Nd:YAG at 809nm is less than 2mm, the pump light needs to be focussed near the input surface of the rod. If focussed too near the front surface insufficient absorption will occur, and if focussed too far into the sample, most of the absorption will occur outside the fundamental mode volume. The ray traces show that at a distance of less than 70mm, the focus is forming too far into the sample. Experimentally, close agreement to these predictions was found. The laser output energy was not critically dependent on the distance of the mirror/rod pair, as long as it was within the distances quoted above.

6.2: Characterisation of the Nd:YAG Laser

The short 8cm resonator was constructed, using the various output couplers in turn. The output pulse energy was observed on an oscilloscope connected to the pyroelectric joulemeter and amplifier. In order to calculate output powers, the pulse duration at the various pump powers needed to be recorded, and this was duly performed using a Si photodiode. Example traces are shown in figure 16, which also includes a trace of the diode current pulse for comparison purposes. At threshold, lasing occurs at the very end of the pump pulse as expected, and as the pump power increases, the laser pulse increases in duration. At around twice the pump threshold, the pulse is of length 130µs, and at four times threshold 165µs, agreeing well with the theoretical pulse lengths predicted.

The output pulses consist of a series of relaxation oscillations. The four times threshold pulse of figure 16 shows "beating" as more than one longitudinal mode is present. This was to be expected as there were no intracavity elements present to force single longitudinal mode operation. These oscillations arise due to a perturbation to the gain or loss of the laser, and in the case of a diode-pumped solid-state laser occur due to the sharp rising edge of the rectangular pump pulse. A population inversion builds up rapidly, reaching a value much greater than the threshold inversion, since the cavity photon number at this time is essentially zero. This number now starts to grow rapidly, and a series of spikes occur as the inversion is alternately built up and depleted. In the case of cw pumping, these spikes are followed by exponentially damped quasi-sinusoidal oscillations, which eventually die out as steady-state conditions are attained[22]. Relaxation oscillations occur in lasers where the upper state lifetime is much greater than the laser cavity lifetime. This is the case with the diode-pumped Nd:YAG laser, where the upper state lifetime of 230μs is much greater than the cavity lifetime of less than 10ns with the resonators involved here.

In order to compare theoretical output powers with the experimental results, the former has to be scaled by certain factors as outlined in section 4. These are listed below.

(1) Quantum defect : 809nm/1064nm = 0.76

(2) Transmission of the collecting optics and input dichroic mirror : 0.75

(3) Fluorescence efficiency of the upper laser level : 0.995

(4) Efficiency of pump absorption : 0.95

(5) Output coupling fraction T/(T + L), where T is the output coupling and L is the round-trip intracavity loss measured to be 3.1%

The efficiency of the pump absorption was got by considering the chirp of the pump pulse. Using the data supplied, which stated a linewidth of 1nm and a chirp during 200μs of 2nm, and convoluting with the Nd:YAG absorption profile of figure 2 yields an effective absorption coefficient of $6cm^{-1}$. For a 5mm length sample, this gives 95% absorption. Experimental verification of this was obtained by measuring the amount of pump light transmitted by the rod. The intracavity round-trip loss was got by plotting threshold pump power against -lnR, where R is the reflectivity of the output coupler being used. This graph is shown in figure 17. The factor L is found by extrapolating to find the vertical intercept. Note that the threshold pump power used here is that incident on the laser rod, not the total diode power needed to attain threshold.

Knowing the experimental threshold, the theoretical pump power can scaled correctly. Multiplying the theoretical output power data by the scaling factors listed above allows the experimental and theoretical graphs to be plotted together and compared. Figure 18 shows the results when the 4.1% output coupler was used. An optical-to optical slope efficiency of 33% was exhibited, in excellent agreement with the theoretical prediction. The threshold pump power was 330mW. The energy input/output curve also resembles its theoretical equivalent (figure 7). The slope of this curve through the three highest energy points was measured to be 28%. With the 4.1% output coupler, because of the relatively high threshold produced, the available diode power could only

achieve three times threshold pumping. Here the slope of the energy curve has not yet reached the cw limit as given by the power input/output slope efficiency. Figure 19 shows the results for the 8cm resonator with the 0.7% output coupler. The threshold pump power was significantly lower at 165mW, and exhibited a slope efficiency of 12.5%. Analysis of the corresponding energy data reveals a slope efficiency of 13%. Using the 0.7% output coupler, the lower laser threshold allows pumping to six times threshold, which is approaching the cw limit, thus the good agreement between the two. A theoretical slope efficiency of 10% was calculated, which is a fair agreement with the actual results, although not as good an agreement as in the 4.1% output coupling case.

In both cases, the experimental data is greater than the corresponding theoretical values. This immediately suggests an error in the specified calibration of the energy meter or the amplifier used, which had nominal fixed gains of 10,100 and 1000. Another important factor must be taken into account here. Figure 20 shows the transmission of the 5mm Nd:YAG sample around 1.064μm. With ideal antireflection coatings, close to unity transmission would be expected. Instead a reflection loss of 6%, that is, 3% at each end of the rod, is evident. For an uncoated YAG sample, the Fresnel reflection loss at a surface would be 8%, and so the antireflection coating provides some reduction in loss.

With a 3% reflection loss per surface, a 12% intracavity round-trip loss would be expected. However, as stated earlier, this was measured instead to be 3.1% for the 8cm resonator. This highlights the advantage of a short resonator, where reflections from the rod ends are not necessarily lost, but may be reflected back by the cavity mirrors, and so still contribute to lasing, thus reducing the round-trip loss. These multiple reflections raise the possibility of etalon effects setting up between the rod ends and the mirrors which would alter the output coupling and in turn change the value of L experimentally measured. Such an effect depends critically on the alignment of the laser rod relative to the cavity mirrors, and so it is very difficult to take account of this in analysing the results.

To illustrate the benefit of a shorter resonator, the cavity was opened up to a length of 24cm. Using the 0.7% output coupler, the graph in figure 21 was obtained. The threshold was increased from 165mW to 420mW, and the slope efficiency was decreased from 12.5% to 6%. This longer resonator was much harder to align, and back reflection of laser radiation less likely to be effective, thus explaining the overall poorer performance.

The variation in maximum output energy was observed as the diode temperature, hence wavelength, was altered, the result of which is shown in figure 22. Laser action was possible over a wide temperature range, with maximum output available 1°C on either side of the optimum temperature of 25°C. The chirp of the laser diode output helps to "smear out" the sharp absorption features of the Nd:YAG, allowing lasing to occur over the wide range observed.

For an 8cm resonator, with a 5mm Nd:YAG laser medium, the TEM_{00} beam waist radius is 248μm. Hence the spot size within the Nd:YAG laser medium is at least 500μm. The focussed pump pulse has a maximum dimension of 500μm, so there is a good overlap between the two. Using the Cohu camera and the beam diagnostic software, the spatial profile of the Nd:YAG output was recorded. At 30cm distance from the output coupler, a spot of $1/e^{-2}$ width 475μm was observed (figure 23) confirming TEM_{00} operation. Assuming that the beam waist at the output coupler has radius 248μm, the half-angle beam divergence can be calculated as 1.35mrad. This gives a beam waist divergence product (BWDP) of 0.34mm.mrad. In order to check this result, the far-field beam divergence was looked at by focussing the laser output through a lens. From this focus, taken to be the new beam waist position, the resultant half-angle divergence was found to be 1.36mrad from a waist of 255μm. Hence the BDWP was found to be 0.35mm.mrad, agreeing well with the near-field result. For a TEM_{00} Gaussian, the BDWP is given by λ/π, which for 1.064μm has the value 0.34mm.mrad. Hence a diffraction-limited TEM_{00} pulse train is generated by this diode-pumped Nd:YAG laser. The smallest transverse dimension in the laser cavity is the rod diameter of 5mm, an order of magnitude greater than the 0.5mm laser mode dimension, so that the aperturing effects of the rod are minimal. The fact that the output coupler is plane also helps to reduce the divergence of the laser output. Therefore it is not surprising that the output is indeed diffraction-limited.

The 1.064μm output was unpolarised, as expected since the active ion is in a cubic host lattice.

§7: CONCLUSION

An end-pumped pulsed Nd:YAG laser producing diffraction-limited 1.064μm radiation which used a 1W peak power laser diode as the pump source has been modelled and characterised.

The modelling illustrated that the pump pulse length, being shorter than the lifetime of the upper laser level, affects the 1.064μm output pulse energy markedly, especially close to threshold, but that the output power has a linear cw-type characteristic, due to the rectangular pump pulse linearly supplying excitation above threshold. The experimental results agreed well with those predicted confirming the theory as a valid model of the laser.

Figure 24 shows the input/output curves for the three different output couplings used. Running the laser diode with at least 1A to get maximum diode efficiency implies using the 4.1% output coupler, which gives a DPSSL exhibiting a 33% optical-to -optical slope efficiency. The diode was shown to have an electrical-to-optical efficiency of 30%, and assuming a power supply efficiency of at worst 70%, a figure for the wall-plug efficiency of 7% is obtained. This is not the true value, as the power requirements of the water circulator unit have to be included. However the unit used here had a cooler rating of 1.4kW, vastly more than required to remove the few watts of heat generated by the diode.

At the CLEO '91 conference, an end-pumped Nd:YAG laser with an optical-to-optical slope efficiency of 39% was reported[23]. Commercially available Nd:YAG DPSSLs include a cw device with a threshold of 21 mW and a 39% slope efficiency[24]. Hence the laser described in this report shows a comparable slope efficiency, but exhibits a far higher threshold power. The high threshold power was due to the relatively large 3% round-trip loss caused by the poor antireflection coating on the laser rod. With better coatings the intracavity loss could be made very small, as Nd:YAG is a four-level laser, thus avoiding reabsorption losses, and the scattering loss is very small at $0.002cm^{-1}$. A low loss cavity will have a much smaller threshold power, and this will also improve the slope efficiency since the output coupling (the useful loss) will be a larger fraction of the total loss. By improving the pump light transmission through the collecting optics and input mirror the slope efficiency will also be increased.

temperature the terminal laser level has a negligible population, approximately exp(-10) of the

APPENDIX

Tabulated below is the theoretical data calculated in section 4. Note that all the energy and power values are normalised to the corresponding threshold. Data was obtained up to eight times threshold, which is greater than could be achieved experimentally.

Pump	Output Energy	Output Power	T1/μs	Tlas/μs
1.000	0.0000	0.000	200.000	0.000
1.050	0.0087	0.116	185.000	15.000
1.100	0.0136	0.100	172.800	27.200
1.200	0.0478	0.200	152.300	47.700
1.300	0.0956	0.300	136.200	63.800
1.400	0.1532	0.399	123.300	76.700
1.500	0.2183	0.500	112.700	87.300
1.600	0.2885	0.600	103.800	96.200
1.700	0.3635			
1.800	0.4413	0.799	89.600	110.400
1.900	0.5225			
2.000	0.6053	1.000	78.900	121.100
2.500	1.0436	1.499	60.800	139.200
3.000	1.5052	2.000	49.500	150.500
3.500	1.9781	2.501	41.800	158.200
4.000	2.4585	3.000	36.100	163.900
4.500	2.9437	3.500	31.800	168.200
5.000	3.4315	3.999	28.400	171.600
5.500	3.9227	4.501	25.700	174.300
6.000	4.4142	4 999	23.400	176.600
6.500	4.9080	5.499	21.500	178.500
7.000	5.4020	5.999	19.900	180.100
7.500	5.8971	6.498	18.500	181.500
8.000	6.3933	6.999	17.300	182.700

REFERENCES

1. R. NEWMAN "Excitation of the Nd^{3+} fluorescence in $CaWO_4$ by recombination radiation in GaAs", J. Appl. Phys **34** (1963) 437

2. R.N. HALL, G.E. FENNER, J.D. KINGSLEY, T.J. SOLTYS & R.O. CARLSON "Coherent light emission from GaAs junctions", Phys. Rev. Lett. **9** (1962) 366

3. R.J. KEYES & T.M. QUIST "Injection luminescent pumping of $CaF_2:U^{3+}$ with GaAs diode lasers", Appl. Phys. Lett. **4** (1964) 50

4. R.B. CHESLER & D.A. DRAEGERT "Miniature diode-pumped Nd:YAG lasers", Appl. Phys. lett. **23** (1973) 235

5. R.L. BYER "Diode-pumped solid-state lasers", Science **239** (1988) 742

6. M. ROSS "YAG laser operation by semiconductor laser pumping", Proc. IEEE **56** (1968) 196

7. L.C. CONANT & C.W RENO "GaAs laser diode-pumped Nd:YAG laser", Appl. Opt. **13** (1974) 2457

8. H.G. DANIELMEYER & F.W. OSTERMAYER, J. Appl. Phys. **43** (1972) 2911

9. K. IWAMOTO, I. HINO, S. MATSUMOTO & K.INOUE "Room temperature cw operated superluminescent diodes for optical pumping of Nd:YAG laser", Jap. J. Appl. Phys **15** (1976) 2191

10. D.R. SCIFRES, R.D. BURNHAM & W. STREIFER "High power coupled multiple stripe quantum well injection lasers" Appl. Phys. Lett. **41** (1982) 118

11. Spectra Diode Labs. product catalogue 1991

12. T.Y. FAN & R.L.BYER "Diode laser-pumped solid-state lasers", IEEE J. Qu. Electron. **24** (1988) 895

13. T.Y. FAN "Diode-pumped solid-state lasers", Lincoln Lab. Journal **3** (1990) 413

14. T.S. CHEN, V.L. ANDERSON & O. KAHAN "Measurements of heating and energy storage in diode-pumped Nd:YAG", IEEE J. Qu. Electron. **26** (1990) 6

optically insulating layer between the active stripes. Therefore each stripe represents an

15. T. GRAY & C. FREDERICKSON "Pumping Nd:YAG lasers: lamp or diode array ?", Lasers & Optronics (Nov. 1990)

16. K.C. PENG, L.A. WU & H.J KIMBLE "Frequency-stabilised Nd:YAG laser with high output power", Appl. Opt. **24** (1985) 938

17. T.J. KANE & R.L. BYER "Monolithic, unidirectional single-mode Nd:YAG ring laser", Opt. Lett. **10** (1985) 65

18. B. HENDERSON & G.F. IMBUSCH "Optical Spectroscopy of Inorganic Solids", Oxford Science Publications, 1989

19. W. KOECHNER "Solid-State Laser Engineering", Springer-Verlag, 1988

20. J. WILSON & J.F.B. HAWKES "Optoelectronics: An Introduction", Prentice Hall Int., 1983

21. A.A. KAMINSKII "Laser Crystals", Springer-Verlag, 1981

22. A.E. SIEGMAN "Lasers", University Science Books, 1986

23. S. YAMAGUCHI & H. IMAI "Array laser-diode end-pumped Nd:YAG laser", Tech. Digest, Conference on Lasers and Electro-Optics, 1991, Paper CFC6

24. Spectra Physics 7200Y1 pump module & 7900Y-106 laser head - specified cw with 21mW threshold, and up to 35mW randomly polarised at 1.064μm

FIGURE LIST

Figure 1: Energy Level Diagram of Nd:YAG Crystal

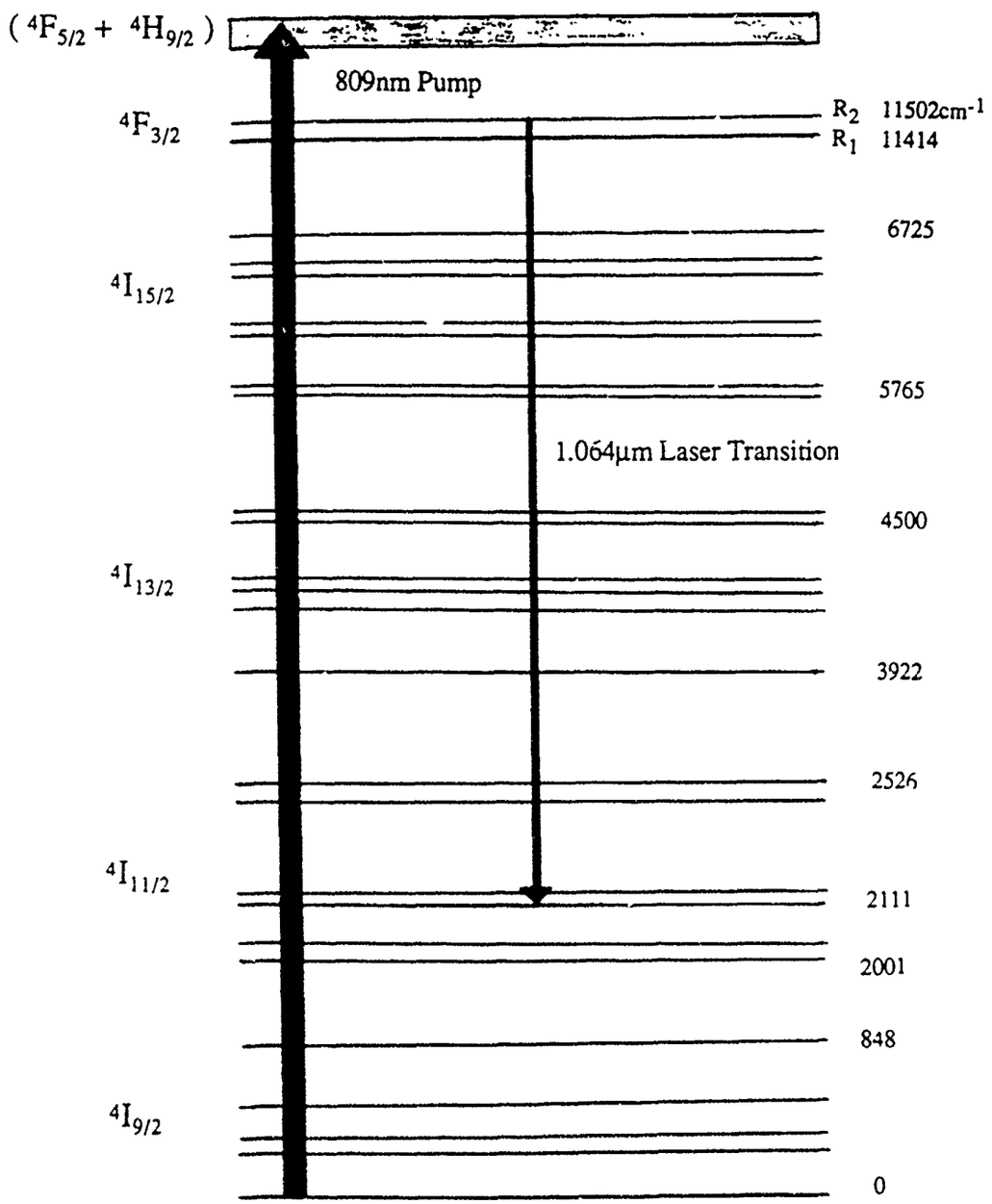

Figure 2: Absorption Spectrum of 1% doped Nd:YAG

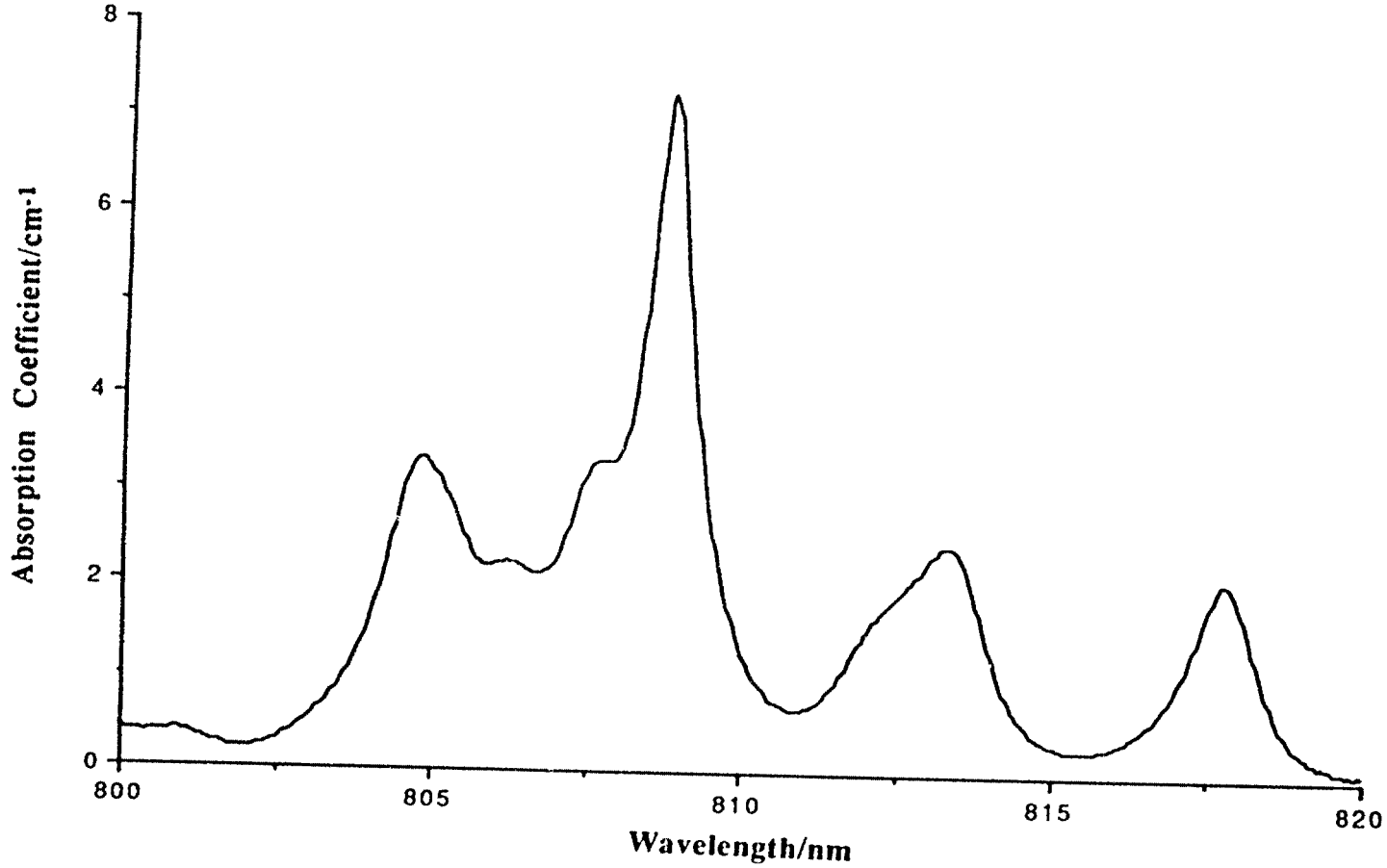

Figure 3: L/I Characteristic Of Laser Diode

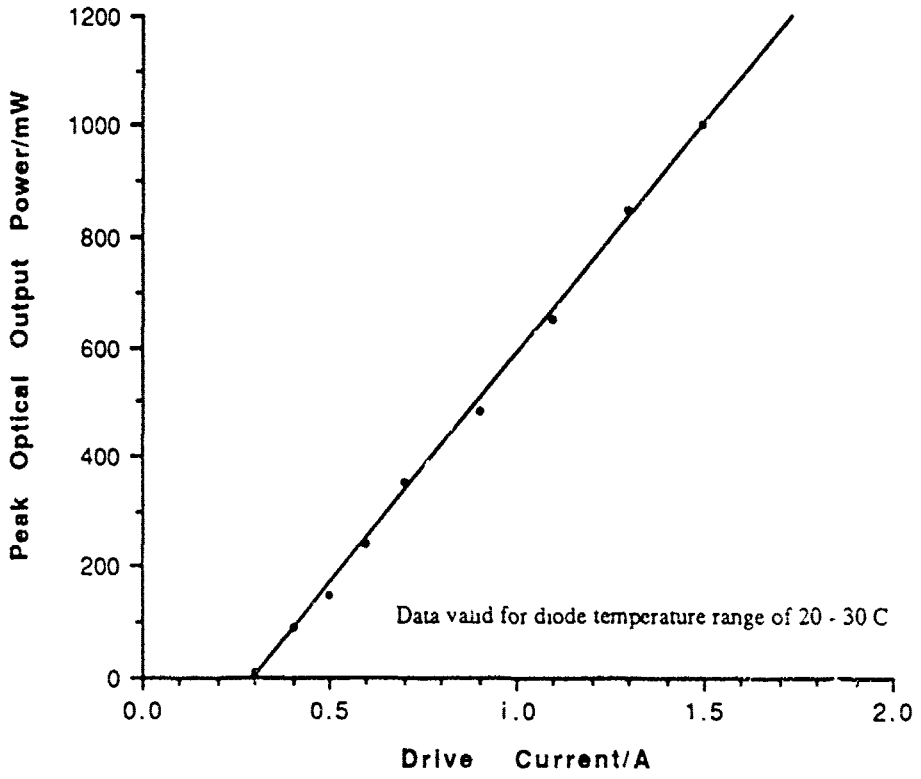

Figure 4: V/I Characteristic of Laser Diode

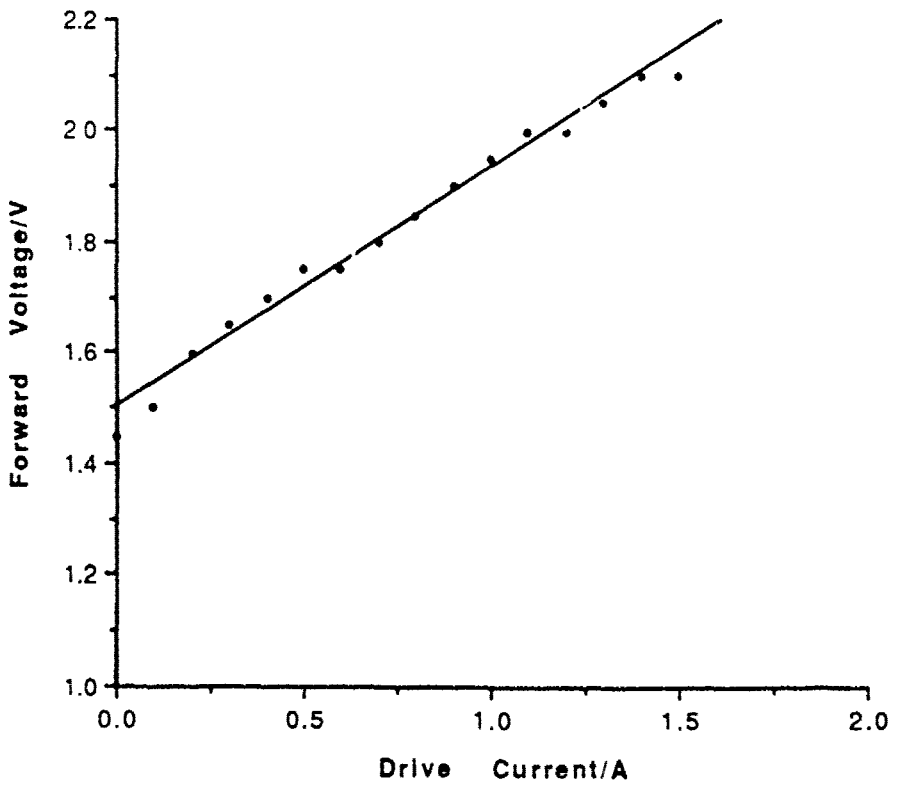

Figure 5: Laser Diode Electrical-to-Optical Power Conversion

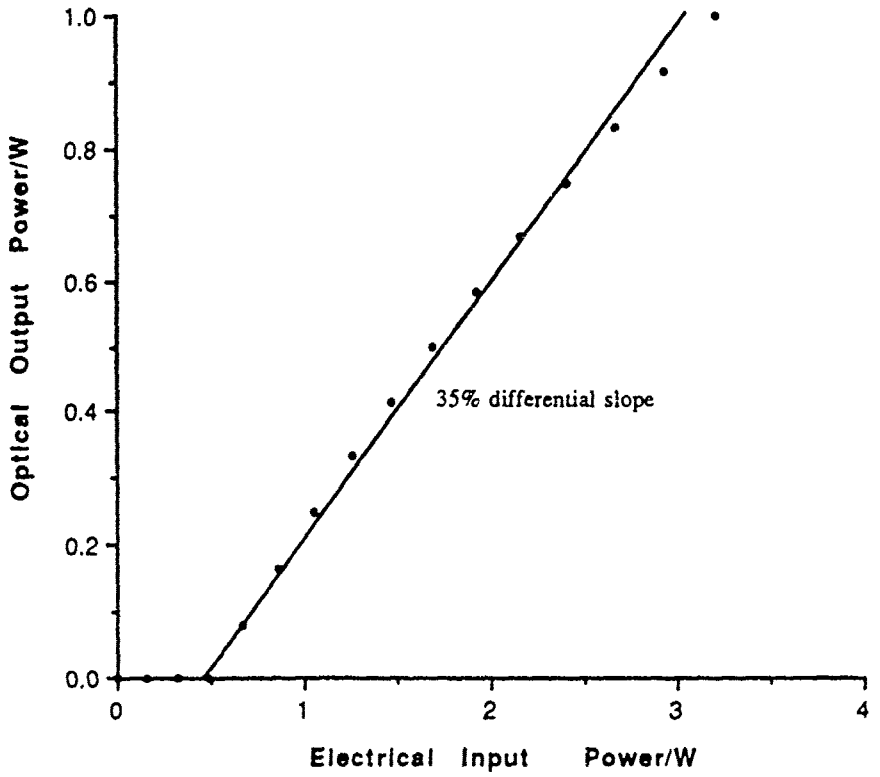

Figure 6: Laser Diode Efficiency as a function of Drive Current

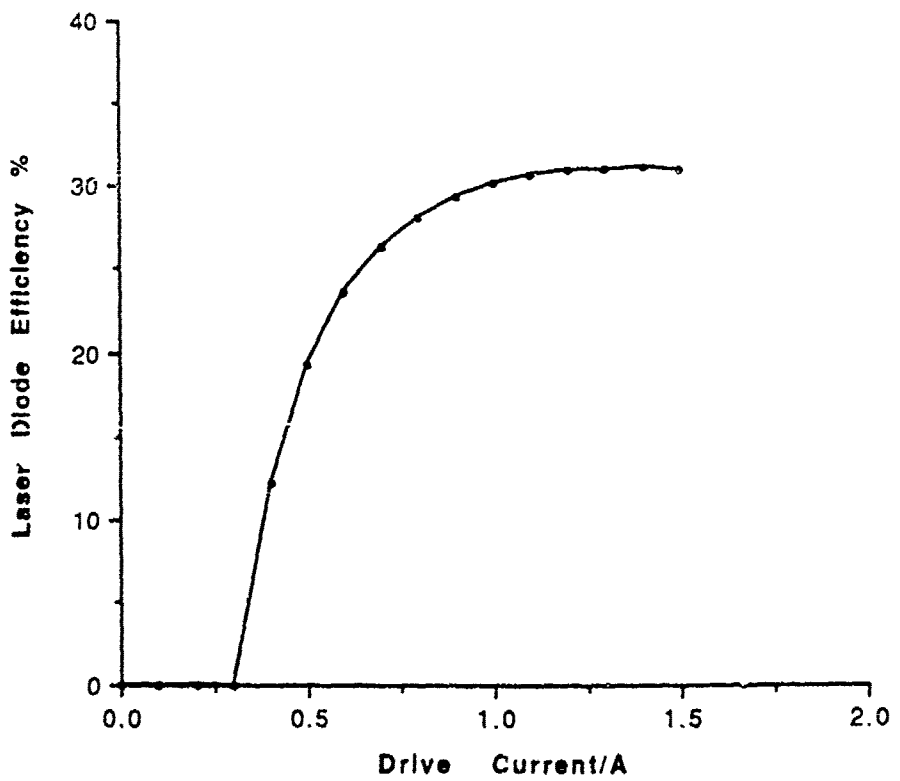

Figure 7: Normalised Optical Energy Input/Output Characteristic

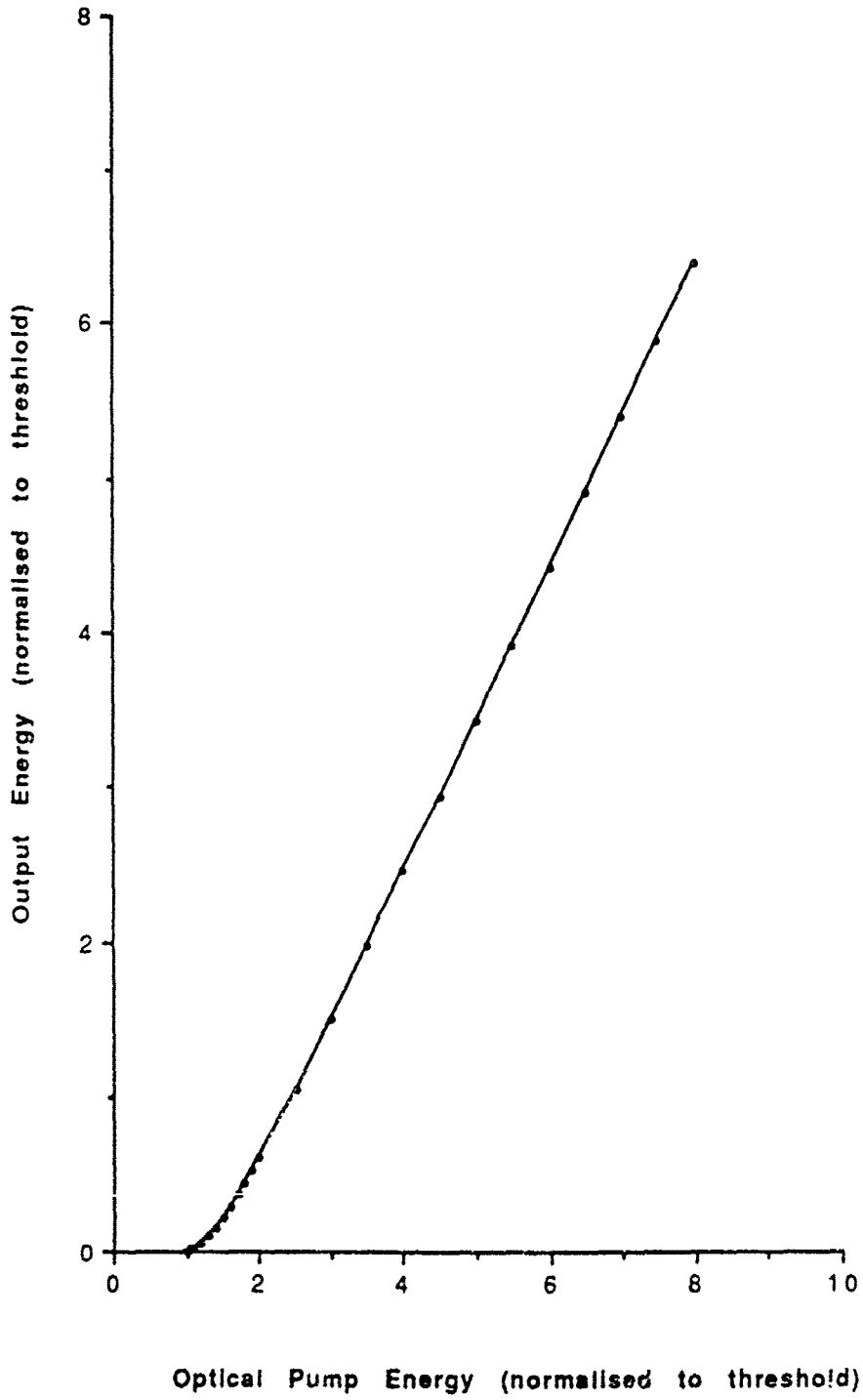

Figure 8: Output Pulse Duration as a function of Optical Pump Energy

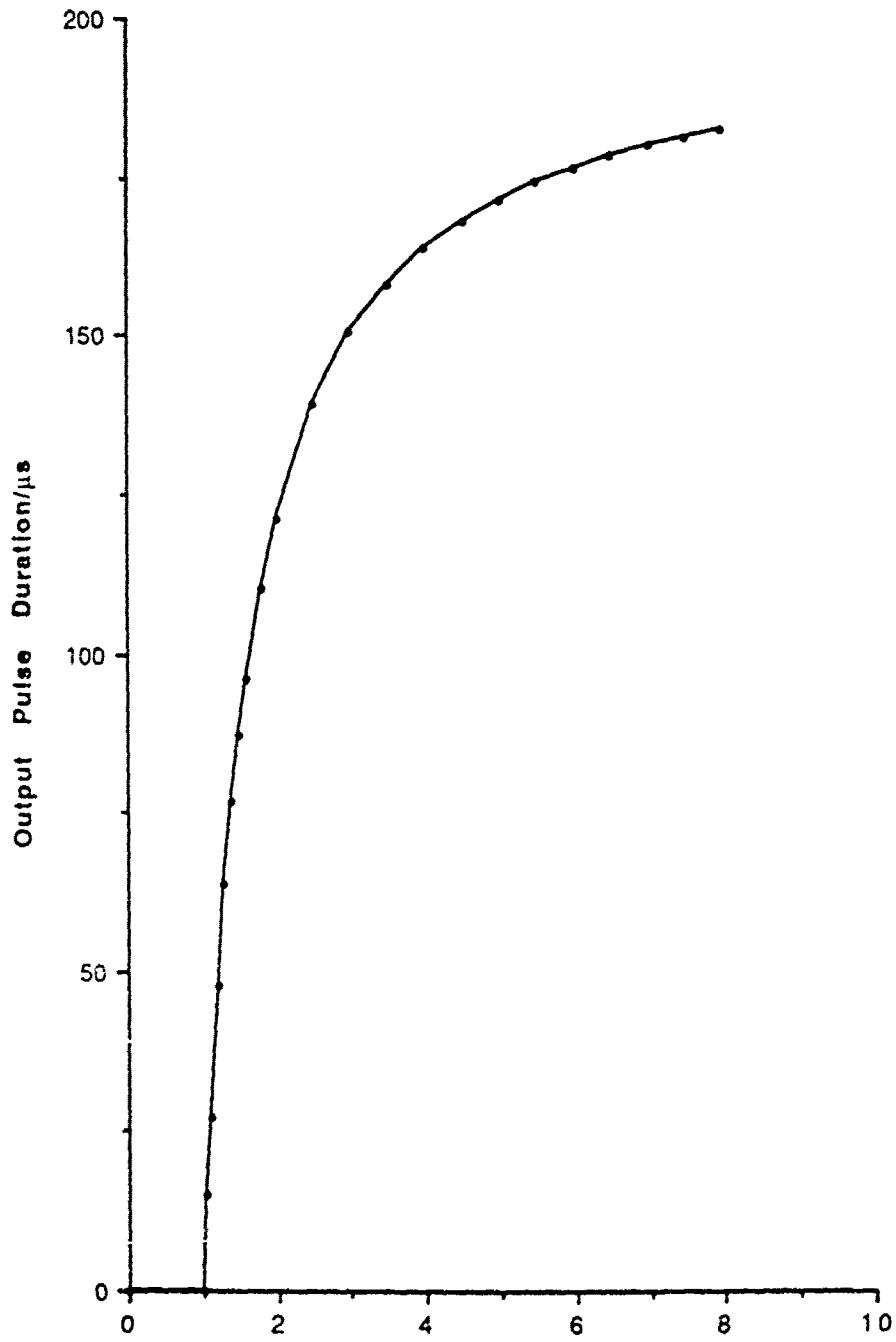

Figure 9: Normalised Optical Power Input/Output Characteristic

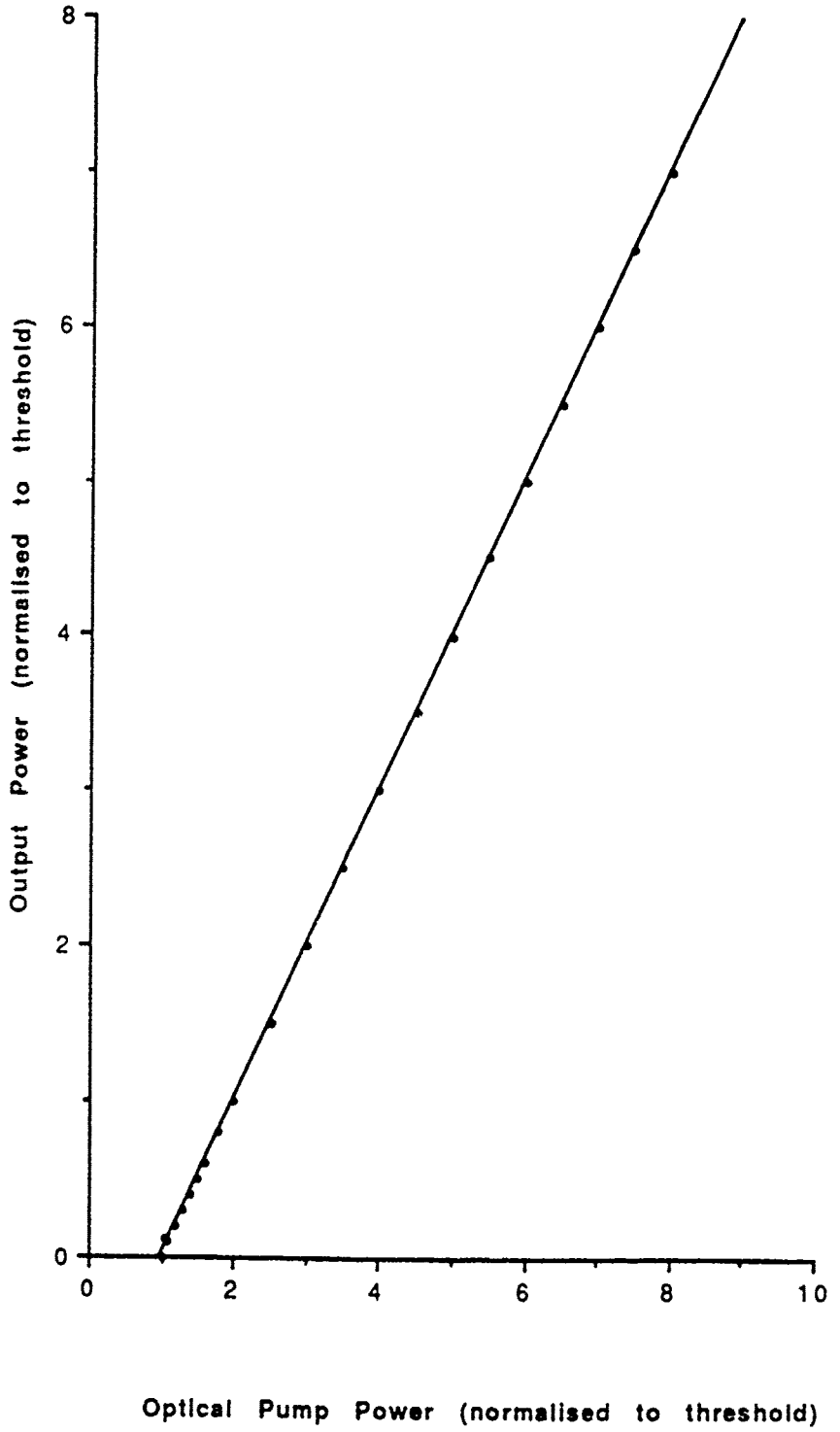

Figure 10: Schematic diagram of the Diode-Pumped Nd:YAG Laser

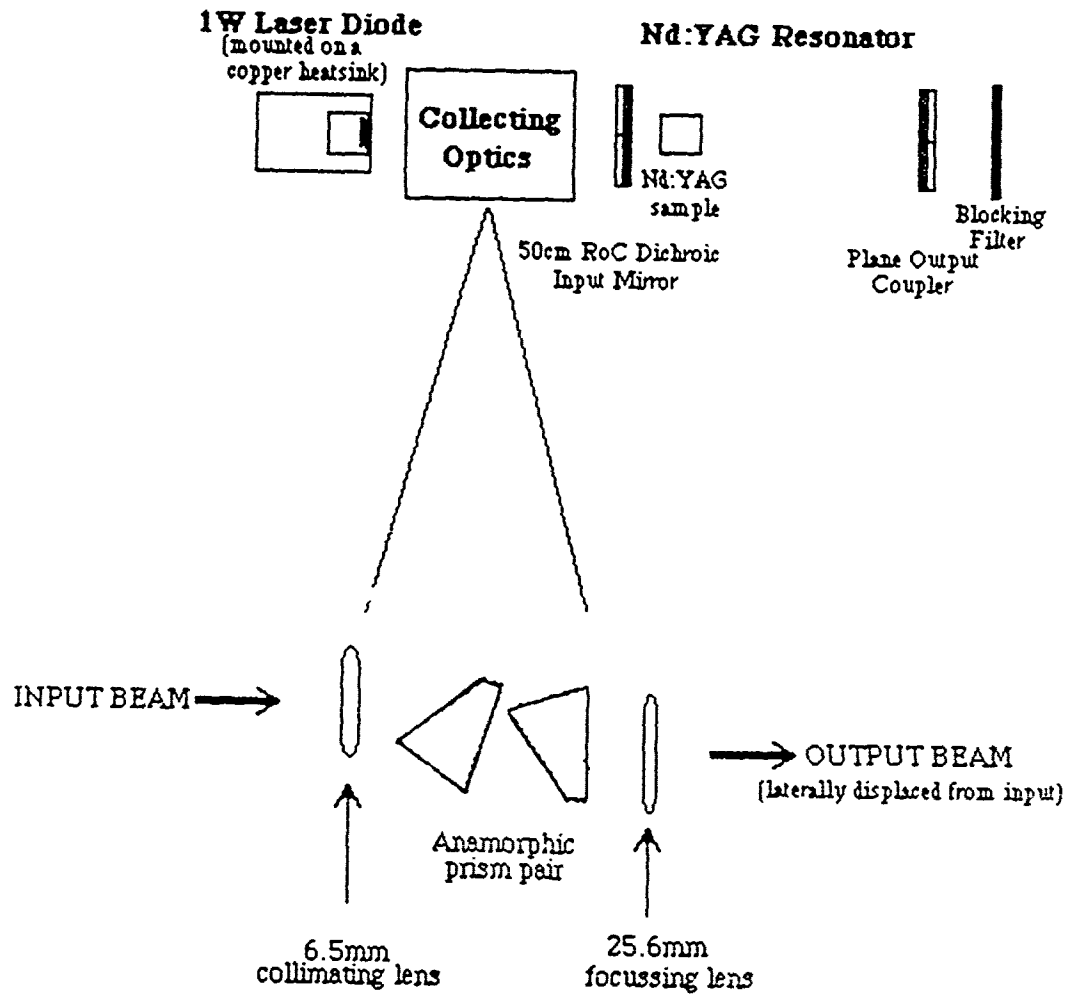

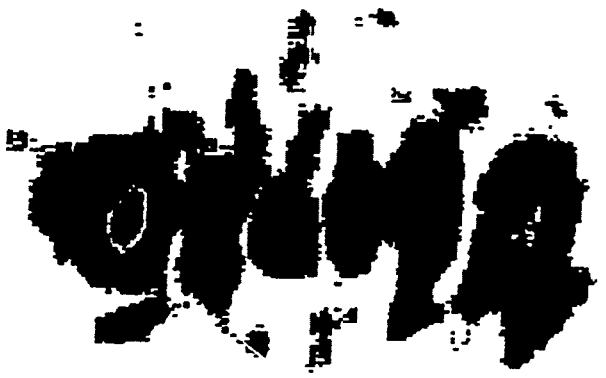

(a) Misaligned cavity showing TEM_{50} operation

(b) TEM_{10} output

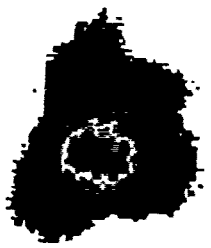

(c) Correctly aligned cavity showing TEM_{00} operation

Figure 11: Change in beam profile as cavity alignment is improved

Figure 12: BEAM4 ray trace (dimensions in mm)

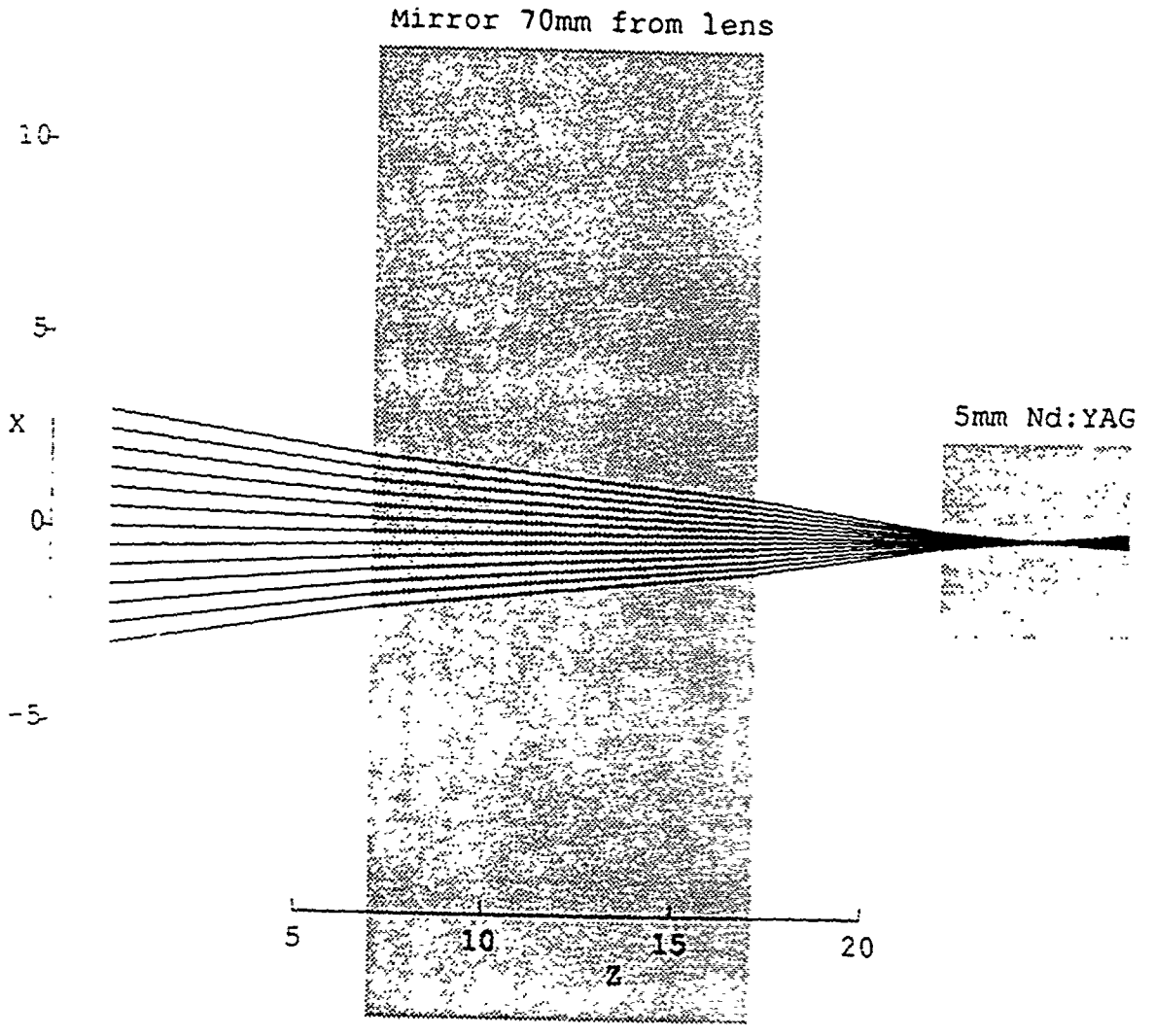

Figure 13: BEAM4 ray trace (dimensions in mm)

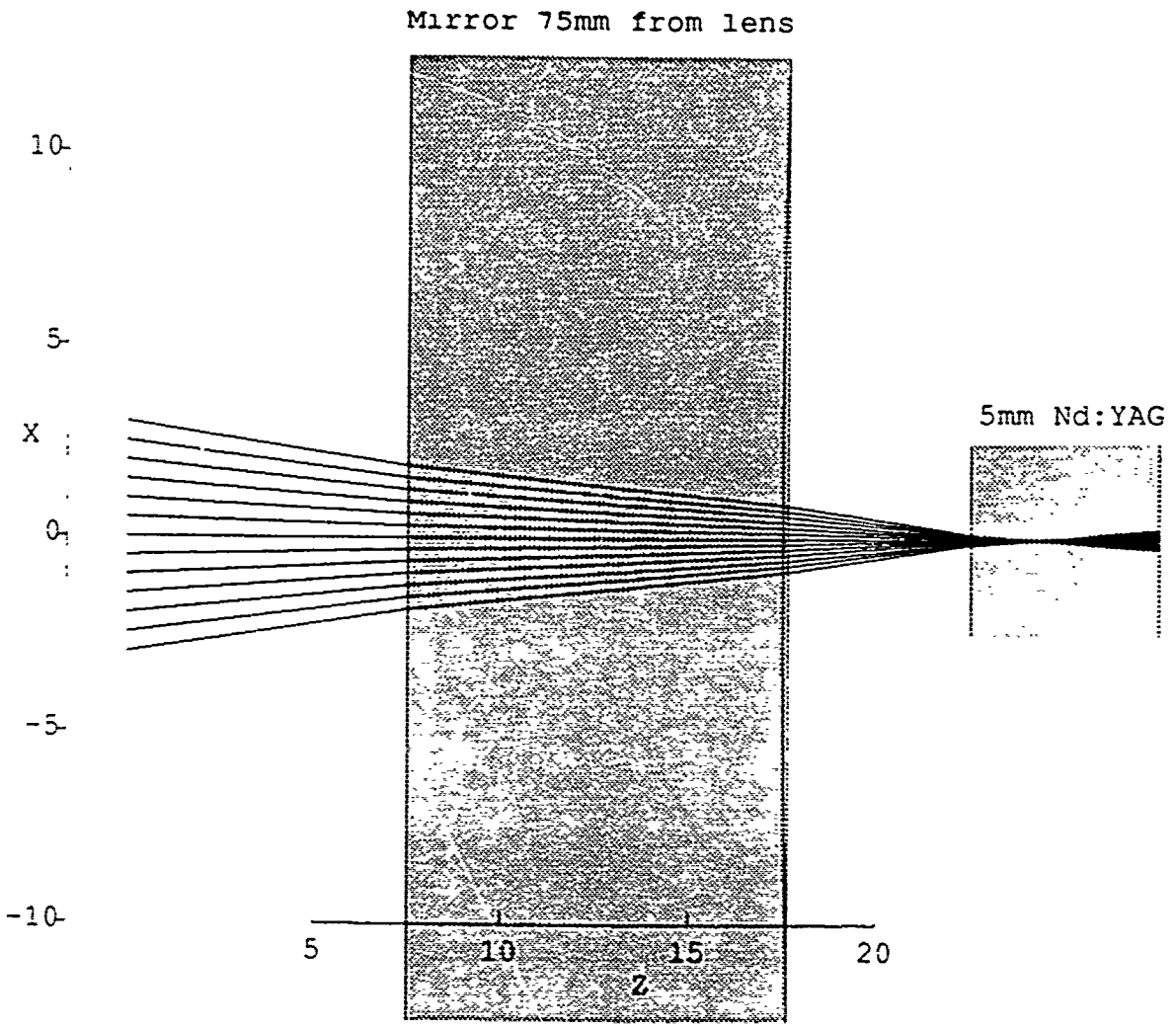

Figure 14: BEAM4 ray trace (dimensions in mm)

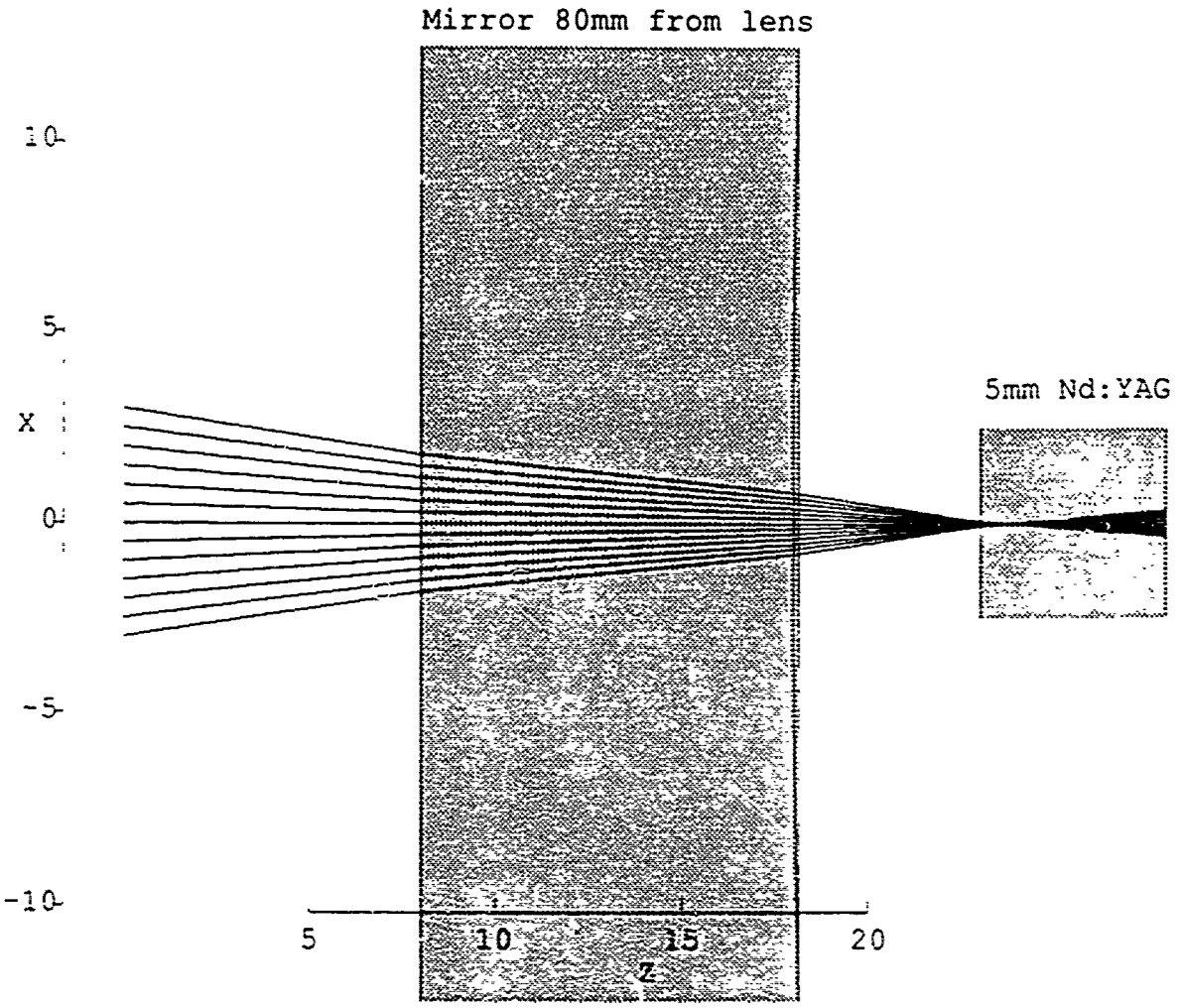

Figure 15: BEAM4 ray trace (dimensions in mm)

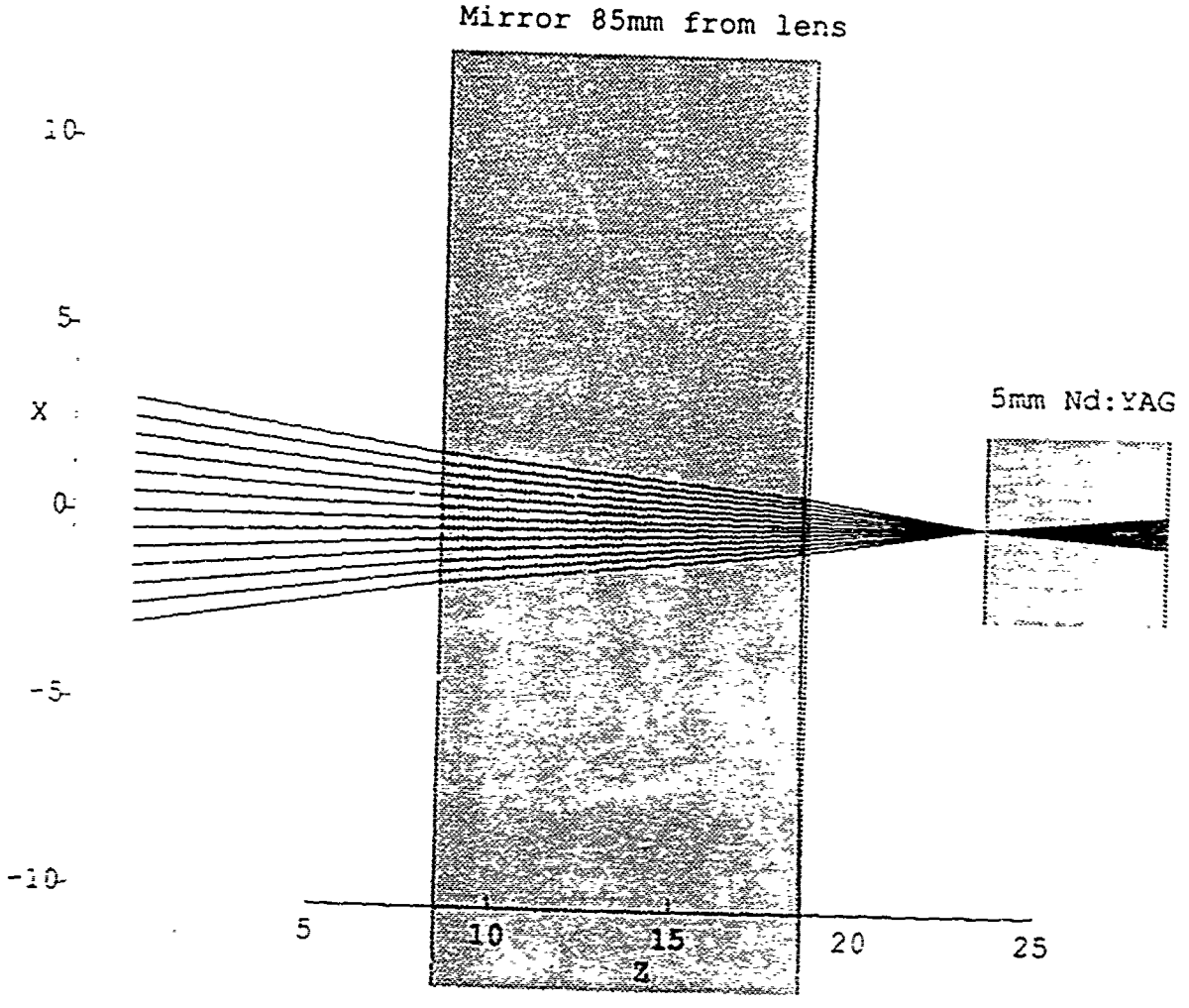

Figure 16: Temporal output of Nd:YAG laser

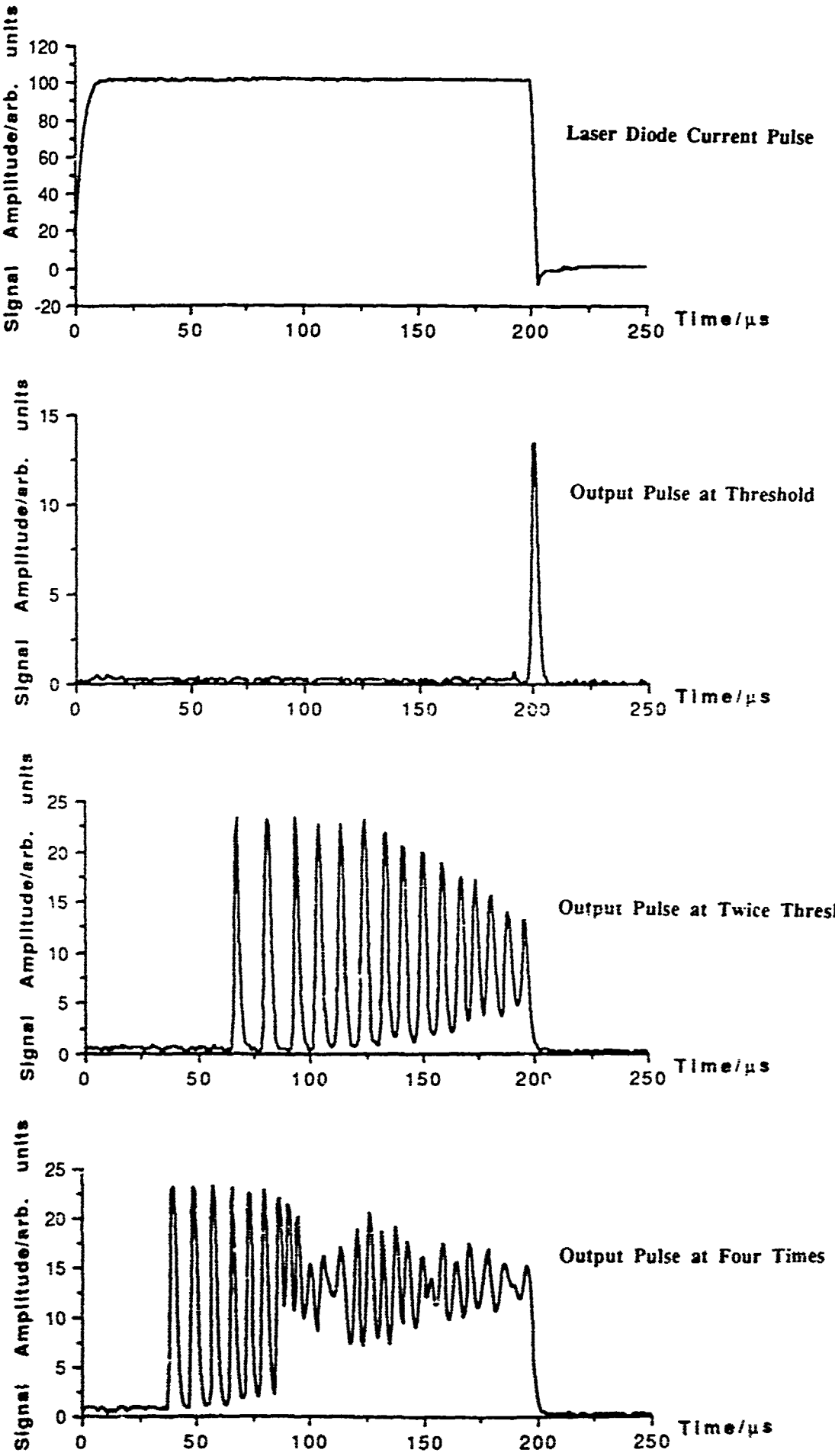

Figure 17: Intracavity Loss Measurement Graph

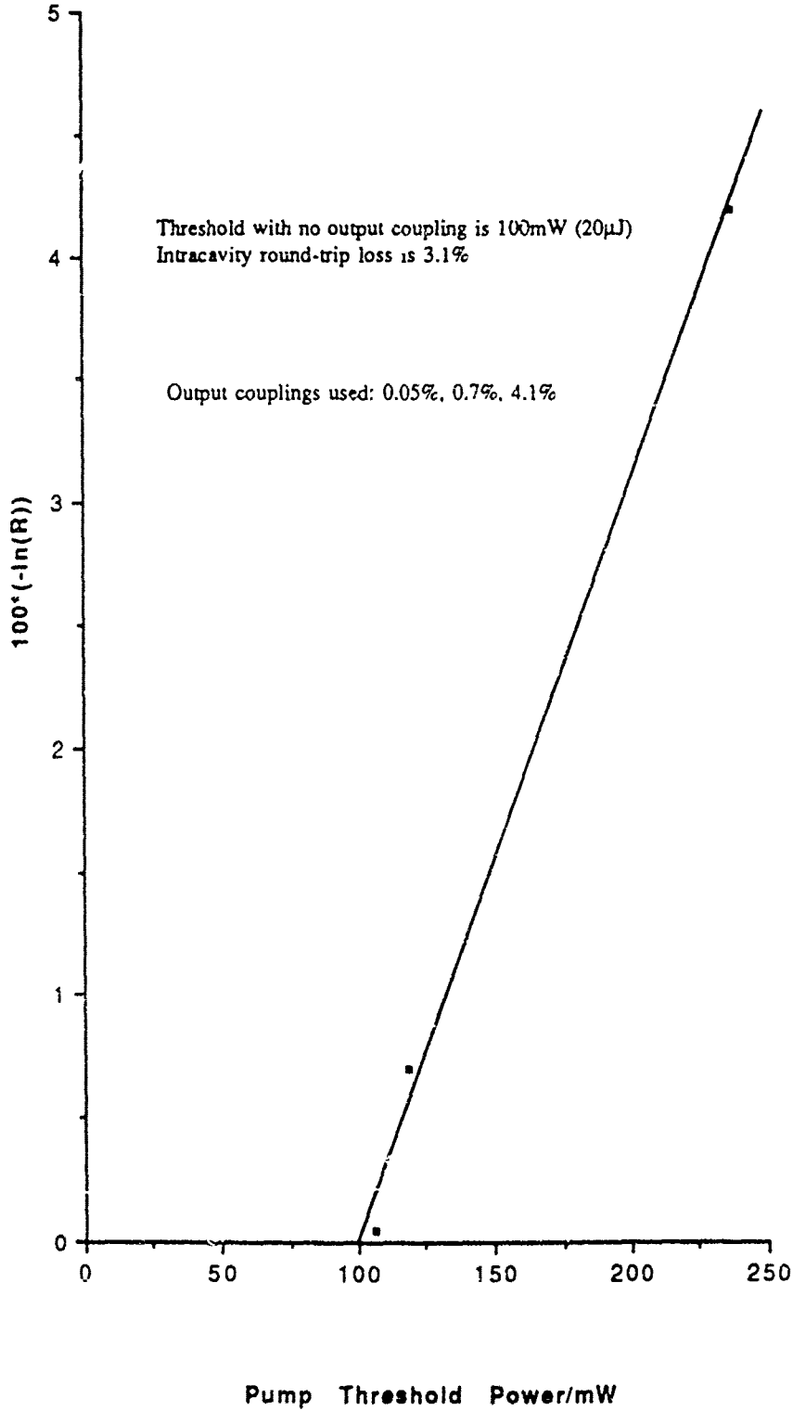

Figure 18: Input/Output Curves with a 4.1% Output Coupler

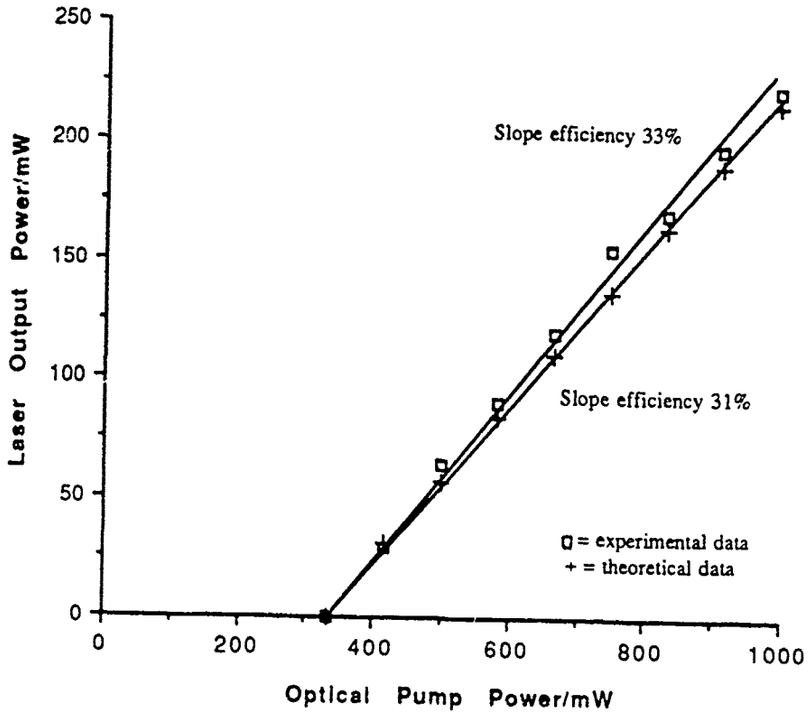

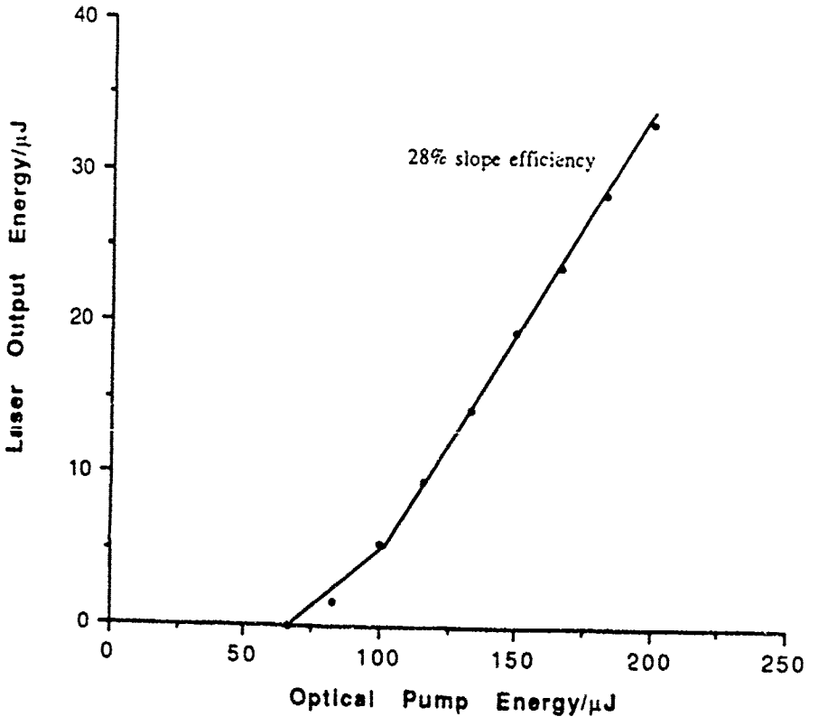

Figure 19: Input/Output Curves with a 0.7% Output Coupler

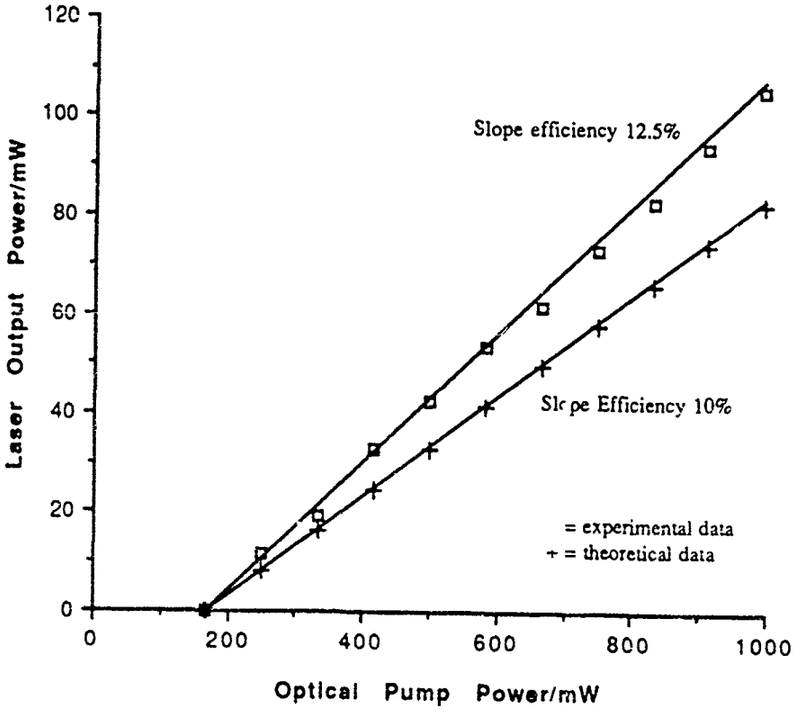

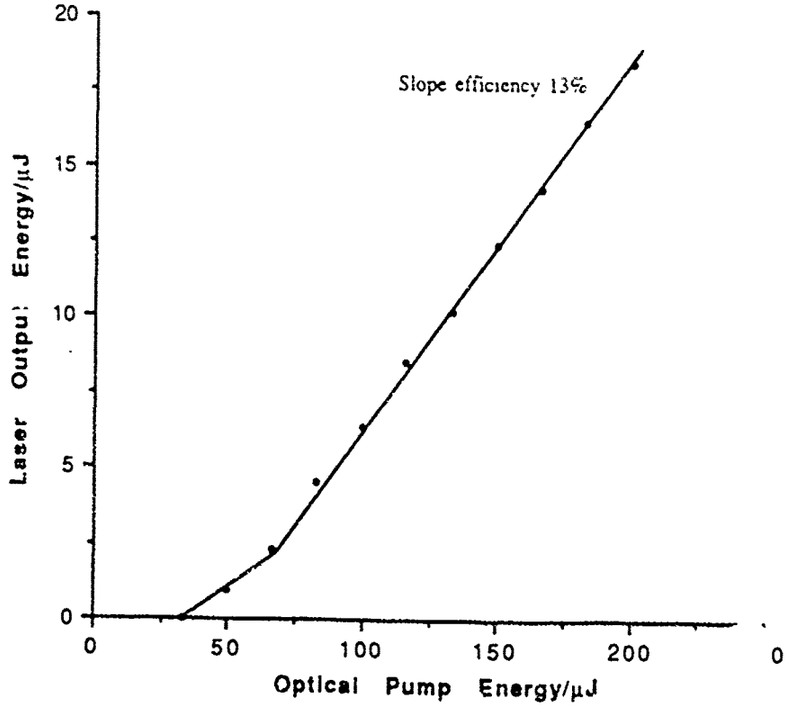

Figure 20: Transmission of the 5mm Nd:YAG sample in the lasing region

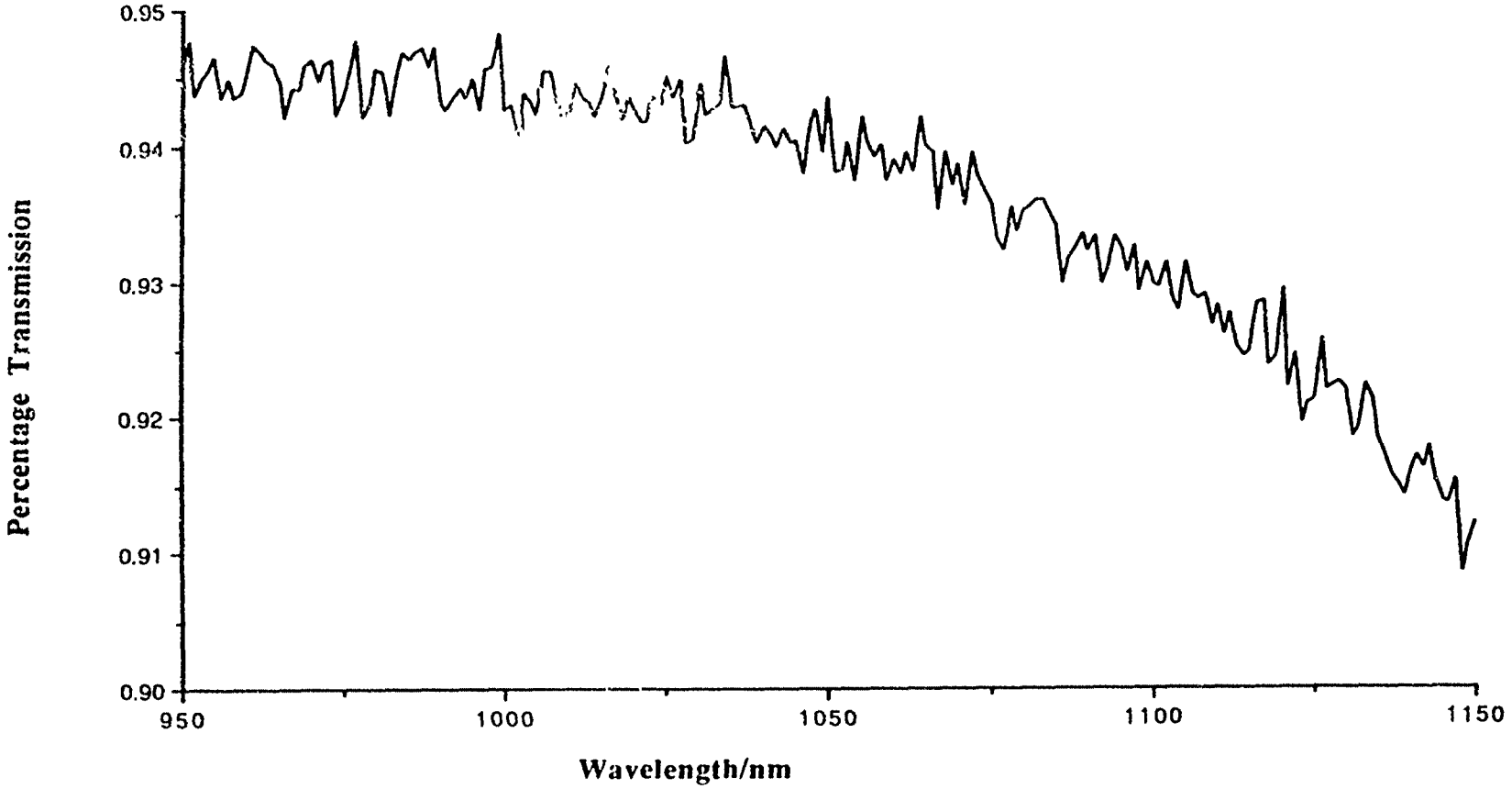

Figure 21: I/O Curves for 24cm resonator with 0.7% Output Coupling

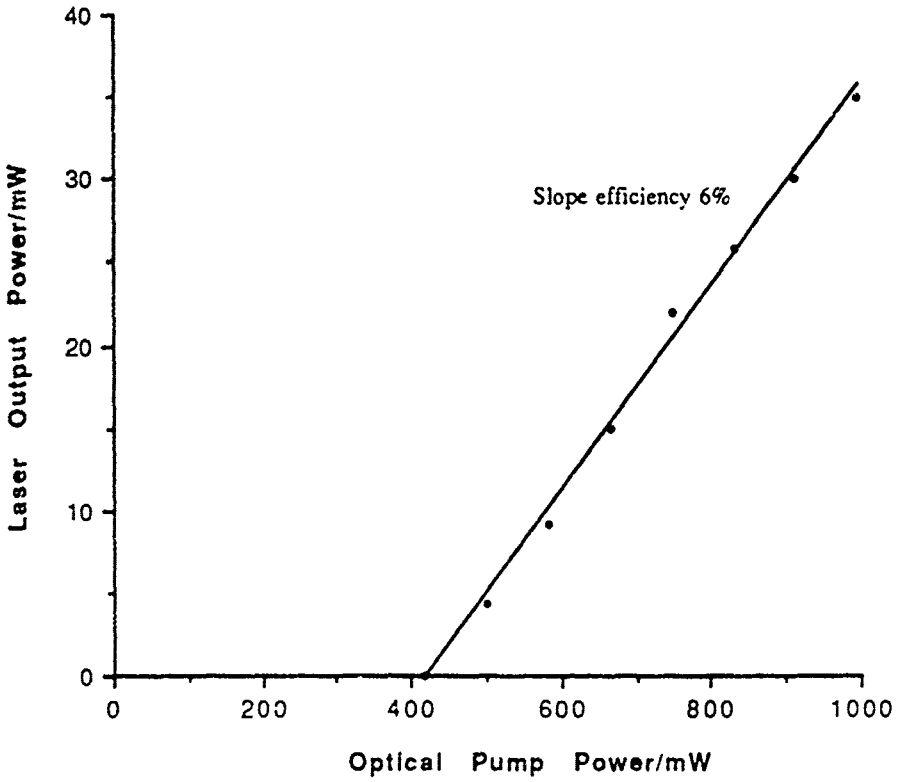

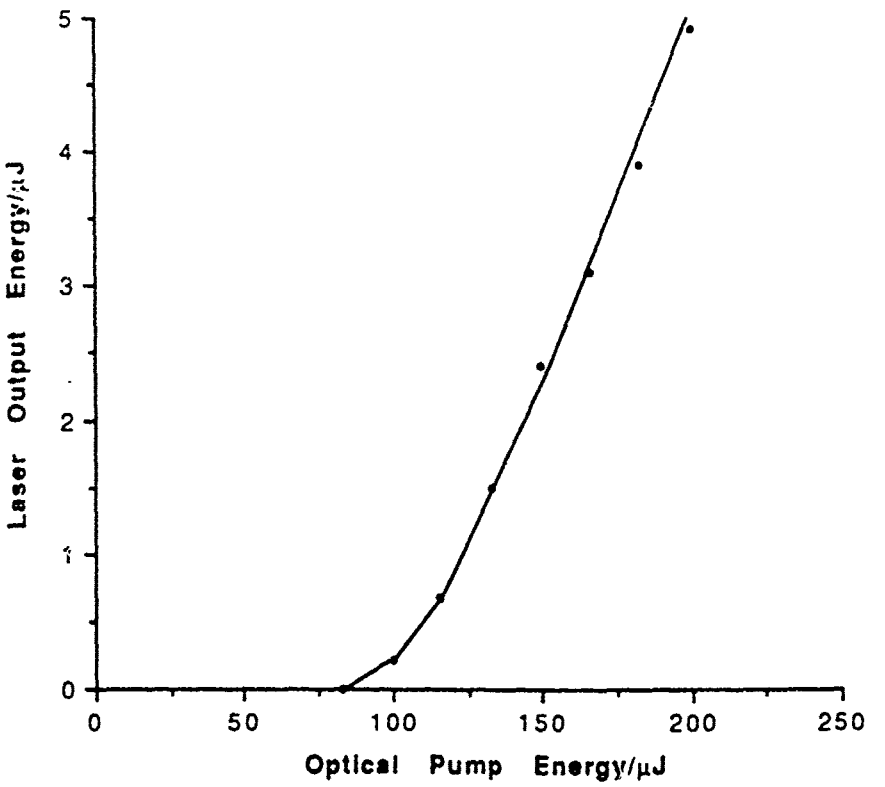

Figure 22: Dependence of Nd:YAG output on laser diode temperature

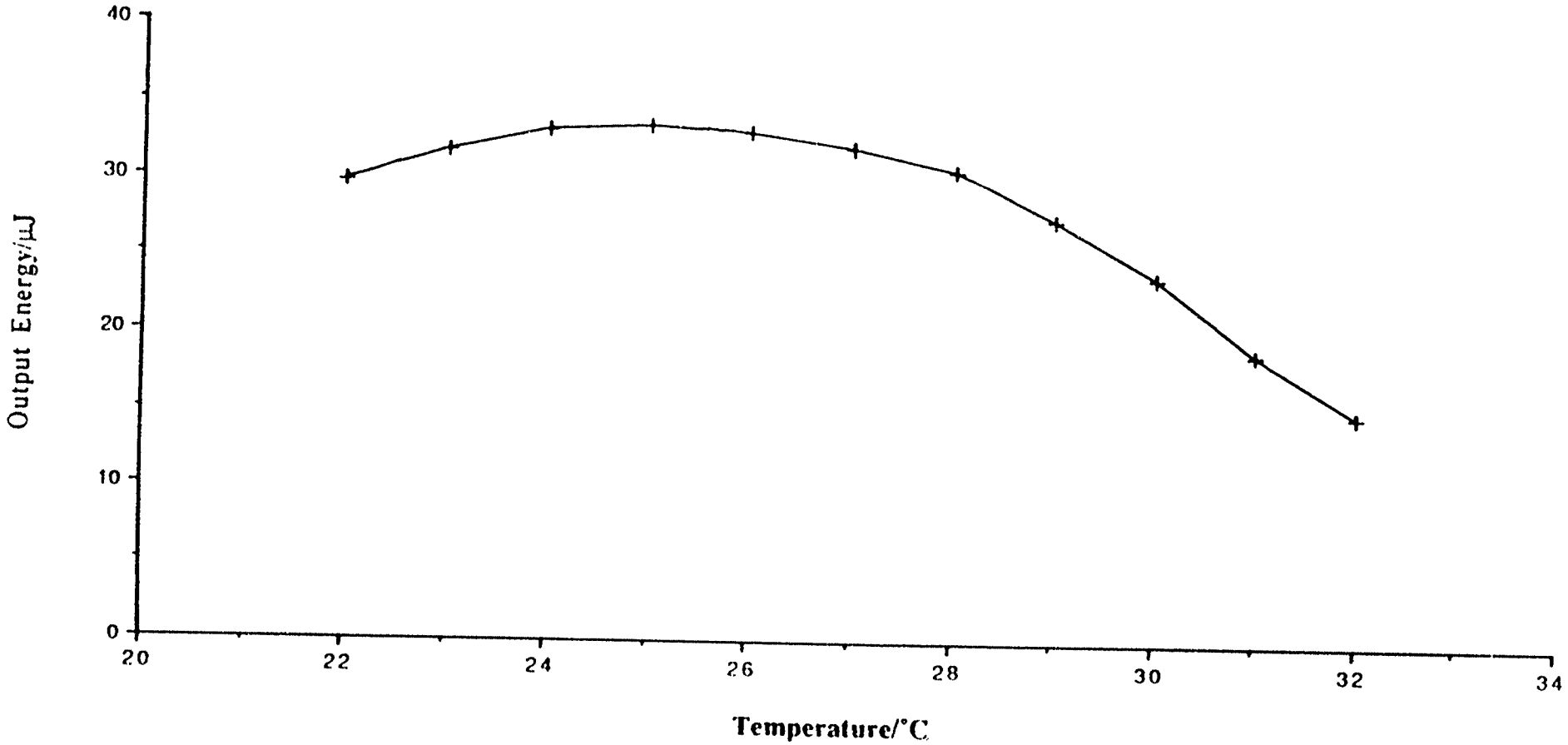

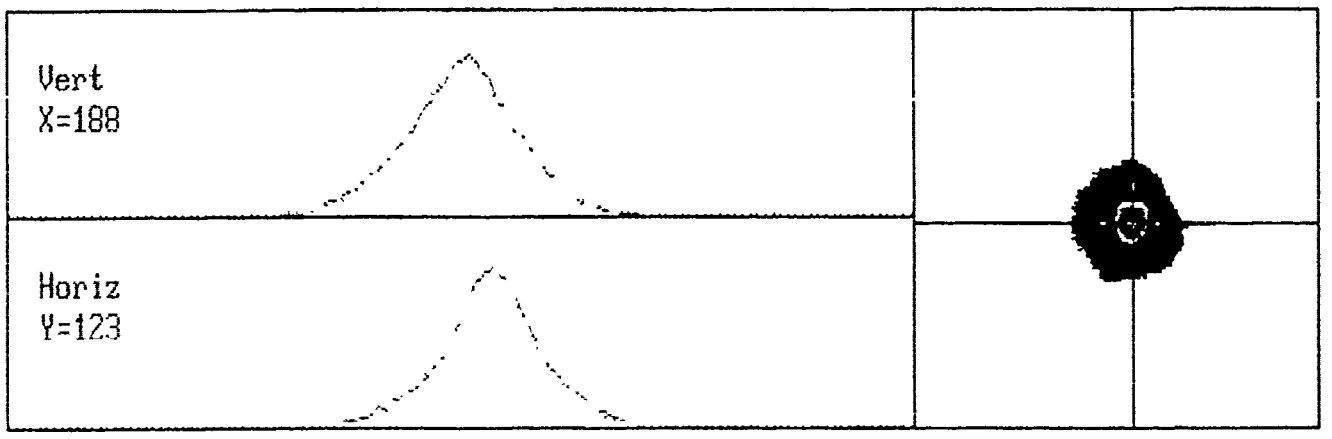

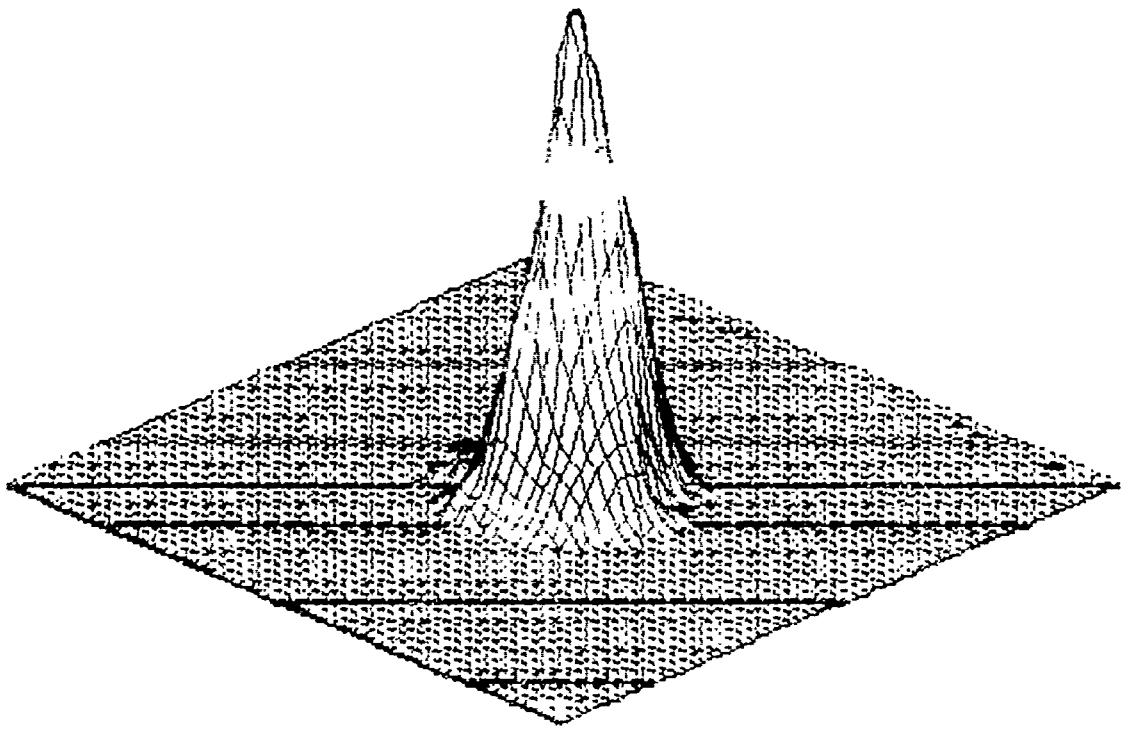

Figure 23: Nd:YAG laser beam profile 30cm from output coupler

Figure 24: Input/Output Curves with various Output Couplings

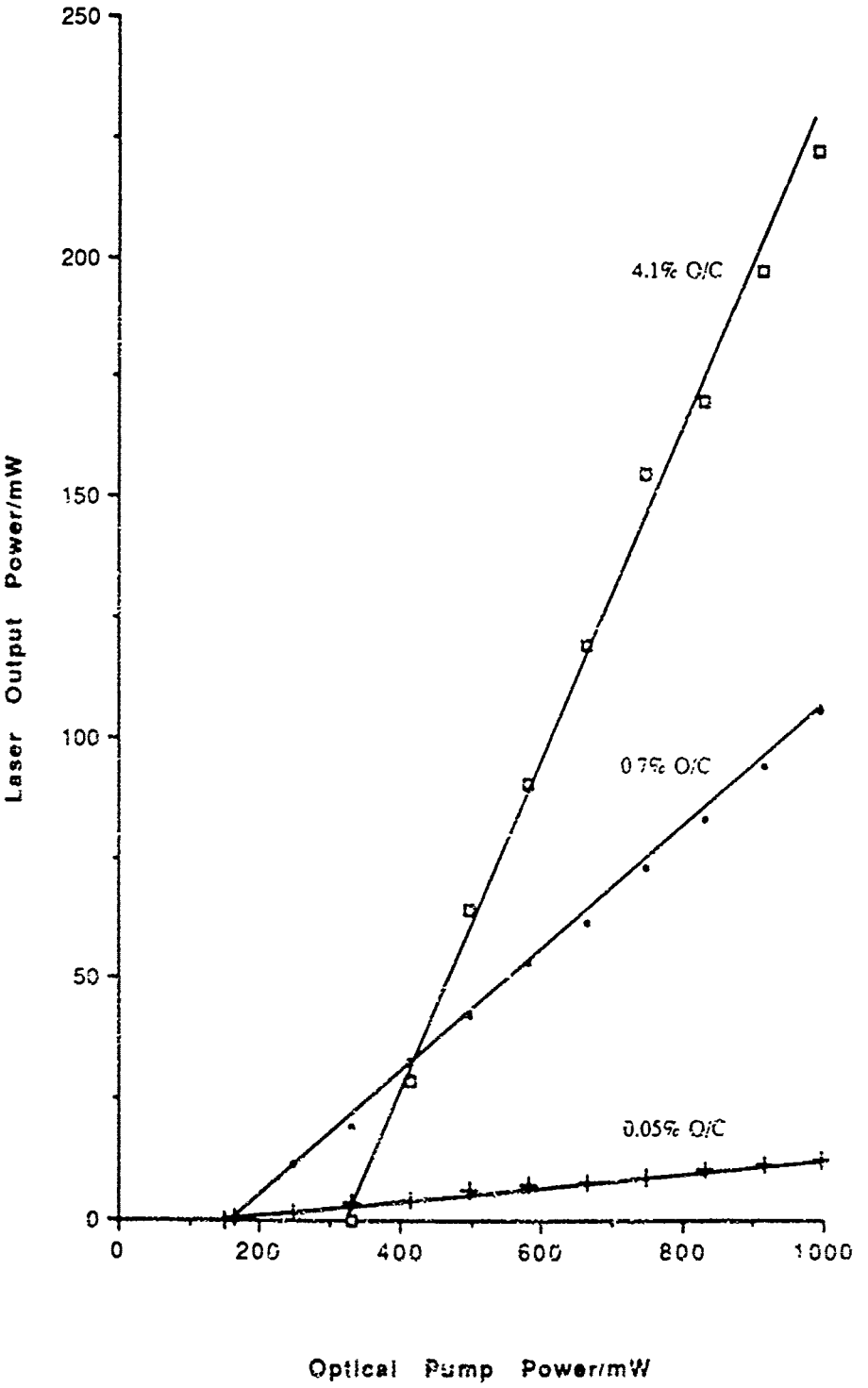

REPORT DOCUMENTATION PAGE

DRIC Reference Number (if known) .....

Overall security classification of sheet .....UNCLASSIFIED.....

(As far as possible this sheet should contain only unclassified information. If it is necessary to enter classified information, the field concerned must be marked to indicate the classification eg (R), (C) or (S).

Originators Reference/Report No.	Month	Year
MEMO 4564	JANUARY	1992

Originators Name and Location
RSRE, St Andrews Road
Malvern, Worcs WR14 3PS

Monitoring Agency Name and Location

Title
LASER DIODE END-PUMPED Nd:YAG LASER

Report Security Classification	Title Classification (U, R, C or S)
UNCLASSIFIED	U

Foreign Language Title (in the case of translations)

Conference Details

Agency Reference	Contract Number and Period

Project Number	Other References

Authors	Pagination and Ref
ELDER, I F	43

Abstract

100 Hz operation of a Nd:YAG laser longitudinally pumped by a 1 W peak power quasi-cw laser diode was investigated theoretically and experimentally. An optical-to-optical slope efficiency of 33%, indicating a wall-plug efficiency of 7%, was exhibited, but the threshold optical power of 330 mW was high due to poor antireflection coatings on the laser rod giving a round-trip intracavity loss of 3.1%. The 1.064 µm output was observed to be diffraction-limited. The theoretical modelling of the laser's input/output characteristics agreed well with the experimentally obtained results.

Abstract Classification (U,R,C or S)
U

Descriptors

Distribution Statement (Enter any limitations on the distribution of the document)

UNLIMITED